16. General Laws of Optical Transitions

16.1 Symmetries and Selection Rules

16.1.1 Optical Matrix Elements

Selection rules and symmetry considerations play a basic role in modern physics. This holds for the atomic shells, the nucleus, elementary particles and for many other areas. We shall present only a small but typical sample here, taking up the perturbation theory discussed in Sect. 15.2. We began with the unperturbed wavefunctions ϕ_n. The perturbation Hamiltonian in one example contained the dipole moment ez. In the following, we shall first choose the x coordinate instead of the z coordinate. We became acquainted with matrix elements of the form

$$H_{mn}^{\mathrm{P}} = \int \phi_m^*(\boldsymbol{r})\, ex\, \phi_n(\boldsymbol{r})\, dV \qquad (16.1)$$

as important parameters. As we observed at that time, there are a number of realistic cases in which matrix elements vanish when the indices m and n are equal, on the basis of symmetry alone. We shall now examine these cases.

16.1.2 Examples of the Symmetry Behaviour of Wavefunctions

As an unperturbed wavefunction, let us consider that of a particle in a box (Sect. 9.1) or of a harmonic oscillator. We recognise (see Figs. 16.1, 2) that these wavefunctions are either "symmetric" or "antisymmetric".

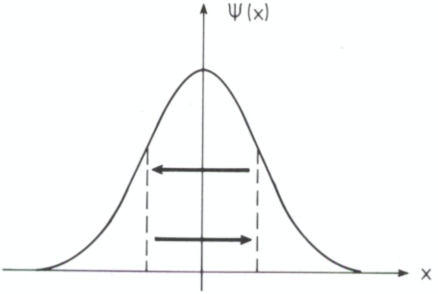

Fig. 16.1. Example of a *symmetric* wavefunction. When reflected through the ψ axis, ψ is converted into itself

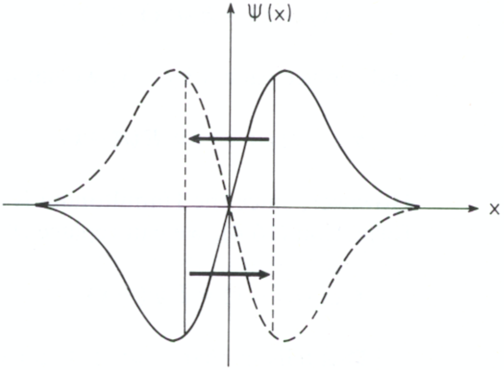

Fig. 16.2. Example of an *antisymmetric* wavefunction. When the wavefunction is reflected through the ψ axis it is transformed into a function with the same magnitude but the opposite sign at each point

A symmetric wavefunction is converted into itself when every x is converted to $-x$. In an antisymmetric wavefunction, this process reverses the sign of the function. We shall now show two things:

1) How this symmetry property of the wavefunction can be derived directly from the Schrödinger equation, without solving it explicitly, and

2) how these symmetry properties can be used to prove that

$$H_{mm}^{\mathrm{P}} = 0 \,. \tag{16.2}$$

We first consider the symmetry properties of the Hamiltonian and select the harmonic oscillator as an example. If we replace x by $-x$, we obviously obtain

$$x^2 \rightarrow (-x)^2 = x^2 \,. \tag{16.3}$$

x^2 is thus unchanged when x is replaced by $-x$, or in other words, x^2 is "invariant" with respect to the transformation

$$x \rightarrow -x \,. \tag{16.4}$$

Since the potential energy of the harmonic oscillator is proportional to x^2, this invariance property naturally applies to the oscillator potential itself:

$$V(-x) = V(x) \,. \tag{16.5}$$

In analogous fashion, one can show that the second derivative with respect to x is also invariant with respect to the transformation (16.4):

$$\frac{d^2}{dx^2} \rightarrow \frac{d^2}{d(-x)^2} = \frac{d^2}{dx^2} \,. \tag{16.6}$$

We can now assume in general that for a certain one-dimensional problem, the Hamiltonian is invariant with respect to the transformation (16.4). If we take the appropriate Schrödinger equation

$$\mathscr{H}(x)\,\psi(x) = E\,\psi(x) \tag{16.7}$$

and replace each x by $-x$, we naturally obtain

$$\mathscr{H}(-x)\,\psi(-x) = E\,\psi(-x) \,. \tag{16.8}$$

However, since the Hamiltonian is supposed to be invariant with respect to the transformation (16.4), we can replace $\mathscr{H}(-x)$ by $\mathscr{H}(x)$ in (16.8),

$$\mathscr{H}(x)\,\psi(-x) = E\,\psi(-x) \,. \tag{16.9}$$

This tells us that if $\psi(x)$ is an eigenfunction of (16.7), $\psi(-x)$ is also an eigenfunction of (16.7). We now make the simplifying assumption that there is only a single eigenfunction for the energy E. The word "single" should be taken with a grain of salt, in that eigenfunctions can differ from one another by a constant numerical factor.

As we see from (16.7) and (16.8), the eigenfunctions $\psi(x)$ and $\psi(-x)$ belong to the energy E. They can differ at most by a constant factor, which we shall call α, due to our assumption above. We thus have the relation

$$\psi(-x) = \alpha\psi(x) . \tag{16.10}$$

If we replace x by $-x$ on both sides of (16.10), the relation becomes

$$\psi(x) = \alpha\psi(-x) . \tag{16.11}$$

We now replace $\psi(x)$ on the right side of (16.10) by $\psi(-x)$ according to (16.11), obtaining as the overall result

$$\psi(-x) = \alpha\psi(x) = \alpha^2\psi(-x) . \tag{16.12}$$

Since we know that ψ does not vanish identically, we can divide both sides by $\psi(-x)$, yielding

$$\alpha^2 = 1 , \tag{16.13}$$

or, taking the square root,

$$\alpha = \pm 1 . \tag{16.14}$$

Inserting this result now into (16.10), we obtain the relation

$$\psi(-x) = \pm\psi(x) . \tag{16.15}$$

This, however, is just the relation we were searching for. As may be seen in Figs. 16.1 and 16.2, the plus sign means that the wavefunction is symmetric, and the minus sign means that it is antisymmetric. We thus see that from the symmetry of the Hamiltonian, it follows automatically that the wavefunctions will have a particular symmetry behaviour.

The argumentation which we have just carried out may be immediately generalised to three dimensions, by utilising consistently the replacement

$$x \to \boldsymbol{r} \tag{16.16}$$

and by replacing the transformation (16.14) by the transformation

$$\boldsymbol{r} \to -\boldsymbol{r} . \tag{16.17}$$

If the Hamiltonian is invariant with respect to (16.17), it follows, in complete analogy to the derivation of (16.15), that

$$\psi(-\boldsymbol{r}) = \pm\psi(\boldsymbol{r}) . \tag{16.18}$$

The transformation behaviour described by (16.18) is denoted as *parity*. If the positive sign is valid, one speaks of positive (or even) parity; if the negative sign holds, the parity is negative (or odd). Correspondingly, the oscillator wavefunctions of Figs. 9.9a, b have positive parity for even $n = 0, 2, 4, \ldots$ and negative parity for odd $n = 1, 3, 5, \ldots$.

Up to now we have assumed that only a single wavefunction (up to a constant factor) belongs to E, or, in other words, that the wavefunctions are not degenerate with one another. It can be shown by the detailed theory that even in the case of degeneracy, the degenerate wavefunctions may be so defined that here, too, the relation (16.18) is fulfilled, as long as the Hamiltonian is invariant with respect to the transformation (16.17).

Before we show by means of symmetry arguments that (16.2) is valid, let us consider another example of a symmetry. Keeping in mind the hydrogen atom problem, which is three dimensional, we investigate symmetry with respect to rotations in three-dimensional space; as a concrete example, we consider a rotation by the angle ϕ around the z axis. We assume, as is for example fulfilled in the hydrogen atom, that the Hamiltonian remains unchanged when we rotate the coordinate axes through the angle $\phi = \phi_1$ about the z axis (Fig. 16.3):

$$\mathscr{H}(r, \phi + \phi_1) = \mathscr{H}(r, \phi) , \tag{16.19}$$

where we have not shown the constant angle θ as an argument.

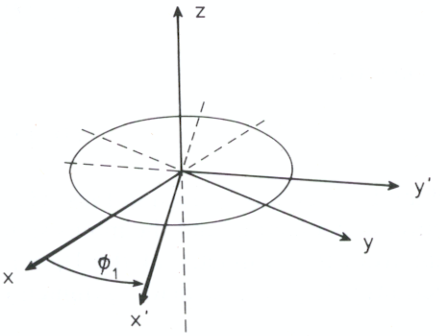

Fig. 16.3. Rotation of the coordinate system around the z axis by an angle ϕ_1

If, in the corresponding Schrödinger equation, we replace ϕ everywhere by $\phi + \phi_1$, we obtain

$$\mathscr{H}(r, \phi + \phi_1)\, \psi(r, \phi + \phi_1) = E\, \psi(r, \phi + \phi_1) , \tag{16.20}$$

or, using rotational invariance,

$$\mathscr{H}(r, \phi)\, \psi(r, \phi + \phi_1) = E\, \psi(r, \phi + \phi_1) . \tag{16.21}$$

Since the wavefunction which occurs in (16.21) must be an eigenfunction of the original Schrödinger equation, we must have (without degeneracy) in analogy to the example treated before,

$$\psi(r, \phi + \phi_1) = \alpha_{\phi_1}\, \psi(r, \phi) . \tag{16.22}$$

Here the constant α can, as we have explicitly indicated, be a function of the angle of rotation ϕ_1. We should like to determine this functional dependence exactly. For this purpose, we write (16.22) again for a second rotation angle ϕ_2:

$$\psi(r,\phi+\phi_2)=\alpha_{\phi_2}\psi(r,\phi)\,. \tag{16.23}$$

We imagine now that ϕ in (16.22) has been replaced by $\phi+\phi_2$. This gives us

$$\psi(r,\phi+\phi_1+\phi_2)=\alpha_{\phi_1}\psi(r,\phi+\phi_2)\,, \tag{16.24}$$

or, using (16.23) on the right side,

$$\psi(r,\phi+\phi_1+\phi_2)=\alpha_{\phi_1}\alpha_{\phi_2}\psi(r,\phi)\,. \tag{16.25}$$

On the other hand, we could have replaced ϕ_1 in (16.22) on both sides of the equation by $\phi_1+\phi_2$, which would have led immediately to

$$\psi(r,\phi+\phi_1+\phi_2)=\alpha_{\phi_1+\phi_2}\psi(r,\phi) \tag{16.26}$$

(Fig. 16.4).

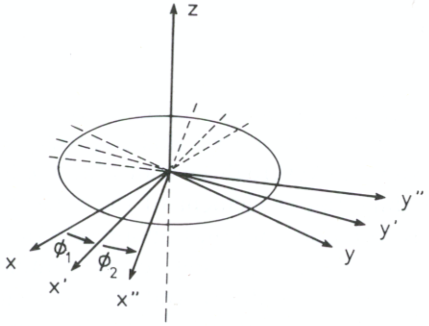

Fig. 16.4. Addition of rotations: two rotations which are carried out one after the other may be replaced by a single rotation

We now compare (16.26) with (16.25). We see immediately that the α's are connected to one another by the relation

$$\alpha_{\phi_1+\phi_2}=\alpha_{\phi_1}\alpha_{\phi_2}\,. \tag{16.27}$$

It may be shown mathematically in an exact way that (16.27) can only be fulfilled by

$$\alpha_\phi=\mathrm{e}^{im\phi}\,, \tag{16.28}$$

where m is still an unknown parameter. (Addition of arguments leads to multiplication of the functions → exponential function.) Now, however, we recognise that every wavefunction must go into itself when we rotate the coordinate system completely around in a circle, that is, when we rotate by an angle of 2π. From this fact, we obtain directly the requirement

$$\mathrm{e}^{im2\pi}=1\,. \tag{16.29}$$

This may be fulfilled by requiring m to be a positive or a negative integer.

To utilise this result, we employ (16.22) again, setting $\phi = 0$ in it:

$$\psi(r, 0+\phi_j) = \alpha_{\phi_j}\psi(r,0) . \tag{16.30}$$

If we leave off the index j and use (16.28), we finally obtain the relation

$$\psi(r,\phi) = \mathrm{e}^{\mathrm{i}m\phi}\psi(r,0) , \quad m \text{ integral} . \tag{16.31}$$

Thus we have found that the wavefunction ψ is dependent on the angle ϕ, and in a way which is in perfect agreement with (10.82), the result which we obtained for the hydrogen atom.

As this example indicates, extremely general conclusions about the structure and the transformation behaviour of wavefunctions may be drawn from symmetry considerations. Naturally, one can also consider rotations around other axes, and rotations around various axes may also be added to give new rotations. The corresponding transformation behaviour of the wavefunctions is treated by what is called the theory of representations of the rotation group, which, however, is beyond the subject matter of this book. We hope, however, that the reader has gained a feeling for the way in which the symmetries of the original problem (i.e. of the Hamiltonian) can lead to a certain transformation behaviour of the wavefunctions.

16.1.3 Selection Rules

We have already met selection rules several times in this book. As we have seen, the coupling of an atom to external fields, especially to the radiation field (light), produces transitions between the electronic states in the atom. However, these transitions only occur (at least in first order) when the corresponding matrix element of the external field, H^{P}_{mn}, is nonzero. If it is zero, the transition is forbidden; we thus obtain selection rules for the occurrence of transitions. We shall now show, using several simple examples, how it follows from the symmetry properties of the wavefunctions that certain matrix elements are identically equal to zero. This is valid independently of the form which the wavefunctions may happen to have.

As a first example we consider an integral which results from leaving out the factor e from the matrix element (16.1). If we replace the functions ϕ_n and ϕ_m by the wavefunction ψ which we are now considering, we have

$$I = \int_{-\infty}^{+\infty} \psi^*(x)\, x\, \psi(x)\, dx , \tag{16.32}$$

where we have chosen a one-dimensional example (for an intuitive picture of this integral, see Fig. 16.5). We rename the variable of integration x, in that we replace x by $-x$:

$$x \to -x . \tag{16.33}$$

The value of the integral naturally remains the same. However, the following individual changes are made in the integral (16.32):

$$I = \int_{+\infty}^{-\infty} \psi^*(-x)(-x)\,\psi(-x)\, d(-x) . \tag{16.34}$$

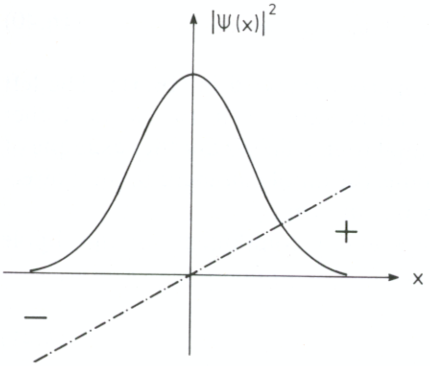

Fig. 16.5. Explanation of the integral (16.32). The integral is obtained by multiplying the value of the function x (– · –) by the value fo the function $|\psi|^2$(—) at each point along the x axis and then integrating the products over all values of x. As can be seen from the diagram, the product for each value of x has the same magnitude as the product for $-x$, but the opposite sign. When added, each pair has a sum of zero, and thus the integral vanishes

By exchanging the limits and accordingly changing the sign of the differential, we obtain

$$\int_{-\infty}^{+\infty} \psi^*(-x)(-x)\,\psi(-x)\,dx\,. \tag{16.35}$$

Now we make use of a symmetry property of the wavefunction, namely the transformation relation (16.15). The transformation (16.4) leaves $\psi^*\psi$ invariant, so that the integral (16.35) differs from the original integral (16.32) only with respect to its sign. We thus obtain the relation

$$I = -I\,, \tag{16.36}$$

which, of course, can only be satisfied by

$$I = 0\,. \tag{16.37}$$

This result is enormously important. It shows us that we have found the value of the integral to be 0 without having done any integrating. We have used only symmetry relationships.

What would have happened if we had calculated a matrix element with different indices m and n? If the perturbation operator were again x, we would then have obtained the following: if ϕ_n and ϕ_m have the same parity, the result is still zero. The integral can only have a non-zero value if the parity of ϕ_n and ϕ_m are different. Here we have the simplest example of a *selection rule*.

As a second example, which is particularly important for atomic shells, we will again consider a dipole matrix element, but now between eigenfunctions of the hydrogen atom. We shall examine a matrix element of the form

$$I_z = \int \psi^*_{n,l,m}(\boldsymbol{r})\, z\, \psi_{n',l',m'}(\boldsymbol{r})\, dV\,. \tag{16.38}$$

In the following, it is useful to employ polar coordinates, in which (16.38) has the form

$$I_z = \int dV\, \psi^*_{n,l,m}(r,\theta,\phi)\, r\cos\theta\, \psi_{n',l',m'}(r,\theta,\phi)\,. \tag{16.39}$$

In order to determine when the matrix element I_z is identical to zero, we again make use of symmetry relationships. This time, however, we consider rotations about the z axis. We allow a rotation through the angle ϕ_0. This converts (16.39) into

$$I_z = \mathrm{e}^{-\mathrm{i}(m-m')\phi_0} I_z\,, \tag{16.40}$$

as one can easily see from the transformation property expressed in (16.31). The left side must naturally remain I_z. Equation (16.40) can be satisfied in two ways. Either $I_z = 0$, or $I_z \neq 0$, but in the latter case m must be equal to m'. This is another example of a selection rule. If the perturbation operator contains the dipole moment in the z direction, a matrix element can only be different from 0 if $m = m'$.

We shall now derive a selection rule for the x and y components of the dipole moment, by considering the integrals

$$I_x = \int dV\, \psi^*_{n,l,m}(r,\theta,\phi)\, x\, \psi_{n',l',m'}(r,\theta,\phi) \tag{16.41}$$

and

$$I_y = \int dV\, \psi^*_{n,l,m}(r,\theta,\phi)\, y\, \psi_{n',l',m'}(r,\theta,\phi)\,. \tag{16.42}$$

We shall multiply the second line by *i* and add it to the first, and also express x and y in spherical polar coordinates. We then obtain

$$I_x + \mathrm{i} I_y = \int dV\, \psi^*_{n,l,m}\, r \sin\theta\, \mathrm{e}^{\mathrm{i}\phi}\, \psi_{n',l',m'}\,. \tag{16.43}$$

If we again carry out a rotation through the angle ϕ_0 about the z axis, we obtain, in complete analogy to the preceding case,

$$I_x + \mathrm{i} I_y = \exp[-\mathrm{i}(m-1-m')\phi_0](I_x + \mathrm{i} I_y)\,. \tag{16.44}$$

From this it immediately follows that

$$I_x + \mathrm{i} I_y = 0 \quad \text{for} \quad m \neq m' + 1 \tag{16.45}$$

and similarly by subtraction of (16.41) and (16.42)

$$I_x - \mathrm{i} I_y = 0 \quad \text{for} \quad m \neq m' - 1\,. \tag{16.46}$$

In summary, if $m \neq m' + 1$ and $m \neq m' - 1$, then

$$I_x = 0 \quad \text{and} \quad I_y = 0\,. \tag{16.47}$$

Here we have discovered another selection rule: I_x or I_y can have non-zero values only when $m = m' + 1$ or $m = m' - 1$.

It can be derived from the rules (16.40, 45 and 46) which transitions in an atom can be induced by a radiation field. If the radiation field is polarised in the z direction, only transitions with $m = m'$ are possible. However, if it is polarised in the x or the y direction, the transitions with

$$m = m' \pm 1 \tag{16.48}$$

are possible. These are the π or σ transitions which were introduced in Sect. 13.3.2.

The selection rule of the angular momentum of the electron,

$$l = l' \pm 1 , \tag{16.49}$$

can be derived from the matrix element (16.38) on the basis of considerations which are similar in principle to the above, but require somewhat more extensive mathematics. The basic matrix element occurs just when light, or more exactly, light quanta, are absorbed or emitted (see also Sect. 16.1.4). Since the total angular momentum of electron and light quantum is conserved, it can be deduced from (16.49) that a quantum of light has the angular momentum (spin) $\hbar$.

We can summarise what has been learned in this chapter as follows: The invariance properties of the Hamiltonian operator lead to certain transformation properties of the wavefunctions. From the transformation properties of the wavefunctions and of the perturbation operator (in the present case this is the dipole operator) it can be rigorously determined which matrix elements vanish identically and which can in principle differ from zero. However, these considerations give no information about the magnitude of the matrix elements, and it can happen that still other matrix elements vanish for other reasons. As it turns out, symmetry considerations allow quite exact predictions, and it is therefore not surprising that such considerations, appropriately generalised, have a basic rôle in the physics of elementary particles.

16.1.4 Selection Rules and Multipole Radiation*

In this chapter we have been primarily concerned with the matrix element

$$\int \phi_n^*(\boldsymbol{r})\, ex\, \phi_m(\boldsymbol{r})\, dV . \tag{16.50}$$

We met this earlier, in Sect. 15.3, where we examined the effect of a light wave on an atom. Conversely, the matrix element (16.50) is also found to apply to the production of light by atomic transitions. Within the limits of this introduction we cannot go into details, but we will describe the basic ideas. As we know from classical electrodynamics, an oscillating dipole generates electromagnetic waves. The dipole is mathematically described by the dipole moment

$$\boldsymbol{P} = -e\boldsymbol{r}(t) \tag{16.51}$$

where $\boldsymbol{r}$ is the vector from the positive charge to the oscillating negative charge. As usual, we assume that the oscillation is purely harmonic, $\boldsymbol{r}(t) = \boldsymbol{r}_0 \sin \omega t$. The dipole moment (16.51) then appears in the Maxwell equations for electromagnetism as a "source term". (For the more interested reader, we can formulate this somewhat more exactly: In the Maxwell equation $\operatorname{curl} \boldsymbol{H} = \boldsymbol{j} + d\boldsymbol{D}/dt$, the polarisation $\boldsymbol{P}$ appears in $\boldsymbol{D}$ if matter, in the present case atoms, is present. In the classical case, this can be expressed by (16.51) or, if several atoms are present, by a summation of several expressions of the form of (16.51).) The question now arises whether there is a quantum theoretical analogue to this source term of the form of (16.51). Let us recall the translation table in Sect. 9.3.4, and accordingly, assign to the classical observable "dipole moment $-e\boldsymbol{r}(t)$" an operator $-e\boldsymbol{r}$ and, finally, the expectation value

$$\int \psi^*(\boldsymbol{r},t)(-e\boldsymbol{r})\,\psi(\boldsymbol{r},t)\, dV . \tag{16.52}$$

What does the wavefunction $\psi(\boldsymbol{r}, t)$ mean here? To obtain an insight, let us imagine an atom with two energy levels E_1 and E_2 and the related wave functions $\phi_1(\boldsymbol{r})$ and $\phi_2(\boldsymbol{r})$. To generate an oscillation, we form a superposition in the form of a "wave packet",

$$\psi(\boldsymbol{r},t) = \frac{1}{\sqrt{2}} \mathrm{e}^{-\mathrm{i}E_1 t/\hbar} \phi_1(\boldsymbol{r}) + \frac{1}{\sqrt{2}} \mathrm{e}^{-\mathrm{i}E_2 t/\hbar} \phi_2(\boldsymbol{r}) , \tag{16.53}$$

where the factors $1/\sqrt{2}$ serve to normalise $\psi(\boldsymbol{r})$. Let us substitute (16.53) in (16.52) and multiply out the individual terms. The result is a sum over expressions of the form of (16.50), in which m and n can take on the values 1 and 2. Let us assume, as above, that

$$\int \phi_1^* e\boldsymbol{r} \phi_1 dV \quad \text{and} \quad \int \phi_2^* e\boldsymbol{r} \phi_2 dV$$

vanish. Then (16.52) takes the form

$$\tfrac{1}{2} \int \phi_1^*(\boldsymbol{r})(-e\boldsymbol{r})\phi_2(\boldsymbol{r})\, dV \cdot \mathrm{e}^{-\mathrm{i}\omega t} + \text{c.c.}^1 , \tag{16.54}$$

where we have also introduced the abbreviation $\omega = (E_2 - E_1)/\hbar$. The expectation value of the dipole moments thus actually oscillates as a classical dipole and generates the corresponding classical electromagnetic field. In this way the relationship between a dipole matrix element and dipole radiation becomes clear.

Now as we know from classical physics, radiation fields are generated not only by oscillating dipoles, but also by other oscillating charge or even current distributions. A loop conducting an electric current acts like a magnetic dipole. If we vary the current in the loop, for example in a sine wave, the magnetic dipole moment oscillates and generates "magnetic dipole radiation". Can such a radiation field also be generated by an *atomic* transition? This is in fact possible, but the matrix element (16.52) or (16.54) is no longer sufficient to describe it mathematically. Instead we must base it on a more exact theory of the interaction between light and electrons.

With the exception of constants, the corresponding part of the Schrödinger equation is

$$e\boldsymbol{p} \cdot \boldsymbol{A} , \tag{16.55}$$

where $\boldsymbol{p} = -\mathrm{i}\hbar\nabla$ is the momentum operator and $\boldsymbol{A}$ is the vector potential of the light field. We have already encountered the interaction expression (16.55) in Sect. 14.1, e.g. in (14.9). There the vector potential referred to a constant magnetic field; here it describes the electromagnetic field. If we express $\boldsymbol{A}$ in terms of plane waves (in complex notation), we have instead of (16.55) expressions of the form

$$e\boldsymbol{p} \cdot \boldsymbol{e}\, \mathrm{e}^{\mathrm{i}\boldsymbol{k}\cdot\boldsymbol{r}} \tag{16.56}$$

in which $\boldsymbol{e}$ is the polarisation vector of the light wave with the wavenumber vector $\boldsymbol{k}$. The matrix element which now appears in perturbation theory,

$$e \int \phi_n^*(\boldsymbol{r}) \boldsymbol{p} \cdot \boldsymbol{e}\, \mathrm{e}^{\mathrm{i}\boldsymbol{k}\cdot\boldsymbol{r}} \phi_m(\boldsymbol{r})\, dV , \tag{16.57}$$

---

[1] Here and in the following, c.c. indicates the complex conjugate of the preceding expression

takes the place of (16.50). Since the wavelength λ is generally large compared to the extent a of the wave function ϕ, we can assume $\boldsymbol{k} \cdot \boldsymbol{r} = 2\pi r/\lambda \ll 1$ and expand the exponential function

$$e^{i\boldsymbol{k} \cdot \boldsymbol{r}} \approx 1 + i\boldsymbol{k} \cdot \boldsymbol{r} + \dots \,. \tag{16.58}$$

If we substitute this in (16.57), the first term is

$$\int \phi_n^*(\boldsymbol{r})\, e\boldsymbol{p} \cdot \boldsymbol{e}\, \phi_m(\boldsymbol{r})\, dV \,. \tag{16.59}$$

In the special case that $\boldsymbol{e}$ is parallel to the x axis and $n = 1$, $m = 2$, we have

$$\int \phi_1^*(\boldsymbol{r})\, e p_x \phi_2(\boldsymbol{r})\, dV \,. \tag{16.60}$$

As is demonstrated exactly in quantum mechanics, (16.60) is identical to

$$-\mathrm{i} m\omega \int \phi_1^*(\boldsymbol{r})\, ex\, \phi_2(\boldsymbol{r})\, dV \quad \text{where} \quad \omega = (E_2 - E_1)/\hbar \,, \quad m\text{: particle mass,} \tag{16.61}$$

or, except for a numerical factor, the familiar dipole matrix element. There are cases of atomic transitions, however, where (16.61) vanishes. (These are "forbidden electric dipole transitions".) Then the matrix element derived from the second term in (16.58),

$$\mathrm{i} e \int \phi_1^*(\boldsymbol{r})(\boldsymbol{p} \cdot \boldsymbol{e})(\boldsymbol{k} \cdot \boldsymbol{r})\, \phi_2(\boldsymbol{r})\, dV \,, \tag{16.62}$$

becomes important. This can also be rearranged (which will not be demonstrated here) and becomes (except for the factor $\omega m\boldsymbol{e}$)

$$\int \phi_1^*(\boldsymbol{r})\, [-e\boldsymbol{r}(\boldsymbol{k} \cdot \boldsymbol{r})]\, \phi_2(\boldsymbol{r})\, dV \,. \tag{16.63}$$

To establish the connection with classical physics, let us think of the integral over $\boldsymbol{r}$ being replaced by a discrete sum over points $\boldsymbol{r}_j$, each with the charge $(-e_j)$. Then

$$(16.63) \to \sum_j (-e_j)\boldsymbol{r}_j(\boldsymbol{k} \cdot \boldsymbol{r}_j) \,. \tag{16.64}$$

However, just this sum appears as the "source term" in the classical theory of electromagnetic fields (it appears as the "Hertz vector"). It is known from this theory that the sum represents a superposition of the electric quadrupole moment and the magnetic dipole moment, the oscillations of which produce the corresponding radiation fields. (In the case of the magnetic dipole, use is made of the fact that $\dot{\boldsymbol{r}} = \mathrm{i}\omega\boldsymbol{r}$.) Thus we recognise a one-to-one correspondence between quantum theory and classical physics with regard to the radiation properties of atoms and classical sources, just as the Bohr correspondence principle requires.

The radiation fields of electric and magnetic dipoles are shown in Figs. 16.6 and 16.7. The theory sketched above, in which the radiation field is treated classically, according to the Maxwell equations, but the "source term" is introduced as a quantum mechanical expectation value, is often referred to in the literature as the "semiclassical" theory.

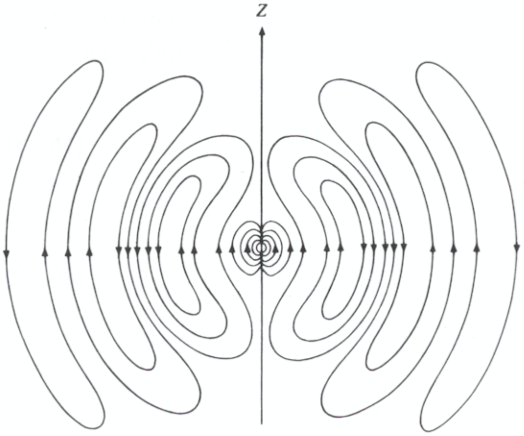

Fig. 16.6. Radiation field for electric dipole radiation. The dipole oscillates in the z direction. The lines connect elements of the electric field $\boldsymbol{E}$ which have the same phase. The radiation field of magnetic dipole radiation is formally the same as that for electric dipole radiation if we replace the electric dipole moment $\boldsymbol{p}$ by the magnetic dipole moment $\boldsymbol{\mu}$ and simultaneously make the substitution $\boldsymbol{E} \rightarrow \boldsymbol{B}$ and $\boldsymbol{B} \rightarrow \boldsymbol{E}$

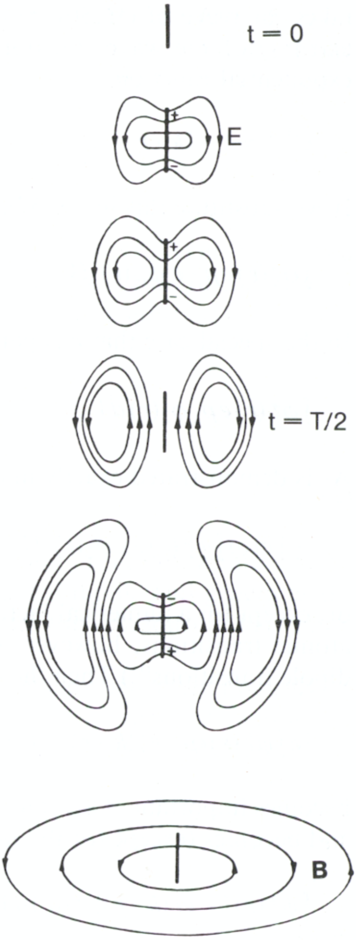

Fig. 16.7. Visualisation of the time dependence of the radiation of a Hertzian dipole. T is the period of oscillation ►

16.2 Linewidths and Lineshapes

As we showed in the Schrödinger theory, electrons can assume certain energy states in the atom. If an electron is in an excited state, it can go from there to an energetically lower state by emitting a quantum of light. The result of this is that the lifespan of the excited state is no longer infinite. In classical electrodynamics, it is shown that the energy of a Hertzian oscillator (= oscillating dipole) decays exponentially with time. Measurements on excited atoms show (Fig. 16.8) that their radiation intensity also decays exponentially. Such behaviour is to be expected, according to the correspondence principle (Sect. 8.11). In fact, the quantum mechanical treatment of radiation, which cannot be given here in detail, shows that the number N of excited atoms decreases according to

$$N = N_0 \, \mathrm{e}^{-2\gamma t} . \tag{16.65}$$

$1/(2\gamma)$ is the time t_0 in which the number N decays to N/e. t_0 is called the lifetime of the state. In the sense of the statistical interpretation of quantum mechanics, (16.65) refers

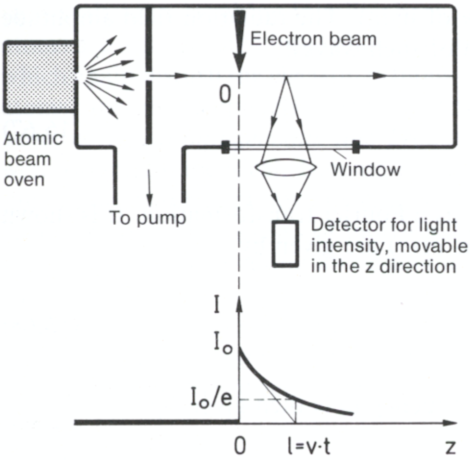

Fig. 16.8. The decay times of excited atomic states can be measured, for example with the arrangement shown here. Atoms in a neutral beam are lifted into defined excited states by irradiation with electrons of the appropriate kinetic energy or with laser light. A movable device for measuring radiation intensity along the line of flight is used. The velocity of the atoms is known, so that the radiative decay of the excited state during the flight through the chamber can be used to calculate the decay time, or lifetime, of the excited state

to the quantum mechanical average which describes the behaviour of many atoms, i.e. of the ensemble. For a single atom, the emission occurs at a completely random time. In analogy to (16.65), the amplitude of the emitted light decreases exponentially. The radiation field amplitude F therefore has the form (Fig. 16.9) in complex notation

$$F(t) = F_0(\mathrm{e}^{-\gamma t + \mathrm{i}\omega_0 t} + \mathrm{c.c.})\,, \qquad t > 0\,. \tag{16.66}$$

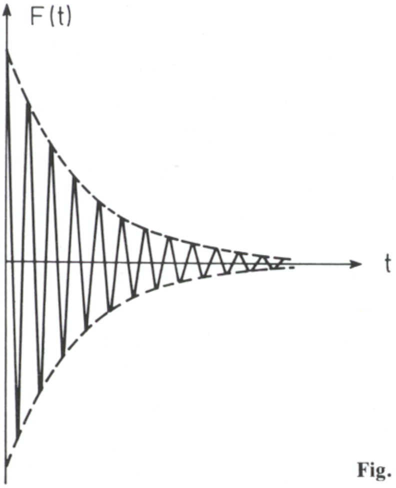

Fig. 16.9. Exponential decay of the radiation field amplitude F (16.66)

Here ω_0 is given by $(E_o - E_f)/\hbar$, where E_o and E_f are the energies of the initial and final atomic states, respectively. F_0 is a real amplitude.

We can imagine that the excitation occurs at time $t = 0$, so that for $t < 0$ there is no light wave. If we use a spectrometer to examine the emitted light, we find that this light is composed of monochromatic components, i.e. waves of the form

$$c(\omega)\mathrm{e}^{\mathrm{i}\omega t} \quad \text{(in complex notation)}\,,$$

where $\omega = 2\pi c/\lambda$ (λ: wavelength, c: velocity of light). The radiation field amplitude (16.66) can be represented as a superposition of such waves:

$$F(t) = \frac{1}{2\pi} \int_{-\infty}^{\infty} c(\omega)\, \mathrm{e}^{\mathrm{i}\omega t} d\omega \,. \tag{16.67}$$

This decomposition is known in mathematics as a Fourier transformation. It is shown in Fourier theory that the Fourier coefficients $c(\omega)$ are given by

$$c(\omega) = \int_{-\infty}^{+\infty} F(t)\, \mathrm{e}^{-\mathrm{i}\omega t} dt \,. \tag{16.68}$$

The intensity of monochromatic light with frequency ω is then given by

$$|c(\omega)|^2 \,. \tag{16.69}$$

For an exponentially decaying light field (16.66), the spectral distribution is thus

$$c(\omega) = -F_0 \left(\frac{1}{\mathrm{i}(\omega_0 - \omega) - \gamma} + \frac{1}{\mathrm{i}(-\omega_0 - \omega) - \gamma} \right) . \tag{16.70}$$

Since $(\omega_0 - \omega) \ll (\omega_0 + \omega)$ and $\gamma \ll (\omega_0 + \omega)$, $(\omega > 0)$, the second term in (16.70) is much smaller than the first and can be neglected. The intensity distribution is then

$$|c(\omega)|^2 = F_0^2 \frac{1}{(\omega - \omega_0)^2 + \gamma^2} \,. \tag{16.71}$$

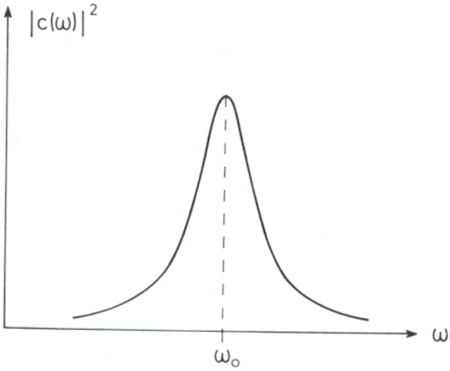

Fig. 16.10. Lorentzian line

A spectral line with the intensity distribution given in (16.71) and shown in Fig. 16.10 is called a Lorentzian line. Its width at half height is given by the atomic decay time t_0 according to $\gamma = 1/(2t_0)$. The linewidth introduced here is also called the *natural* linewidth. Typical numerical values are $t_0 \approx 10^{-8} - 10^{-9}$ s (10^{-8} s $\triangleq 5 \cdot 10^{-4}$ cm^{-1} $\triangleq$ 15 MHz), and thus $\gamma = 10^8 - 10^9\ \mathrm{s}^{-1}$.

It is intuitively reasonable that the electron orbitals of gas atoms can also be disturbed by collisions between the atoms. This constantly causes changes in the resulting light emissions, resulting in a line broadening which is called collision broadening. If atoms are incorporated into solids, they interact constantly with the lattice oscillations, which again disturb the electron orbitals and lead to line broadening. In these cases, the atoms are all completely identical, and the resulting line broadening is "*homogeneous*". "*Inhomogeneous line broadening*" occurs when individual atoms, which were originally identical, become distinguishable through additional physical conditions. For example, atoms in solids can occupy different types of positions within the lattice, so that the energies of individual electrons are differently displaced. These displacements often lie along a continuum and their intensities assume a Gaussian distribution.

Another example of inhomogeneous line broadening is *Doppler broadening* in gases. According to the Doppler principle, the frequency of light emitted by an atom moving toward the observer with velocity v differs from that emitted by an atom at rest by

$$\omega = \omega_0(1 \pm v/c) \,, \tag{16.72}$$

where c is the velocity of light. The frequency is increased when the atoms are moving toward the observer, and decreased when they are moving away. Let us now imagine a gas at thermal equilibrium. According to the Boltzmann distribution (2.8) the number of gas atoms whose velocity components v *in the direction of the observed light wave* lie in the interval $(v, v+dv)$ is given by

$$n(v)\,dv = N\left(\frac{m_0}{2\pi kT}\right)^{1/2} \exp\left(-\frac{m_0 v^2}{2kT}\right) dv \ . \tag{16.73}$$

N is the total number of atoms, k is the Boltzmann constant, T the absolute temperature and m_0 the atomic mass. (The difference between (2.7) and (16.73) is based upon the fact that (2.7) refers to the *three dimensional* motion of the gas atoms, while (16.73) refers to one velocity component v.) Since, according to (16.72), a frequency displacement is associated with the velocity v, we obtain an intensity distribution given by

$$I(\omega) = \text{const} \cdot \exp\left(-\frac{m_0 c^2(\omega_0-\omega)^2}{2kT\omega_0^2}\right), \tag{16.74}$$

as is shown in Fig. 16.11. The total linewidth at half height is given by

$$\Delta\omega_{\mathrm{D}} = \frac{2\omega_0}{c}\left(2\ln 2 \cdot \frac{kT}{m_0}\right)^{1/2} . \tag{16.75}$$

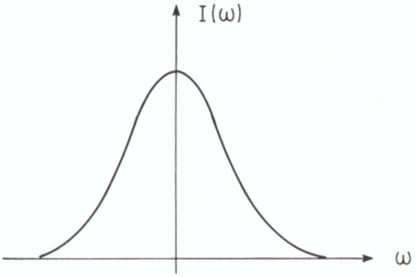

Fig. 16.11. Gaussian line shape

According to (16.75), the Doppler width of a spectral line, $\Delta\omega_D = 2\pi\Delta\nu_D$ is thus proportional to both the frequency and the square root of the temperature. For the yellow D line of sodium, at $T = 500$ K, the Doppler width is $\Delta\nu_D = 1700$ MHz, or $(1/\lambda)_D = 0.056$ cm^{-1}. For optical spectral lines, this width is generally significantly greater than the natural linewidth γ [see (16.71)].

In contrast, the Doppler broadening of microwave or radiofrequency transitions between excited atomic states (which can be studied by double resonance methods, see Sect. 13.3.7) is generally smaller than the natural linewidth. At frequencies $\nu < 10^{10}$ Hz, the Doppler width at the same temperature is, according to (16.75), $<10^4$ Hz. The spectral resolution of such double resonance methods is thus no longer limited by Doppler broadening.

Doppler broadening also occurs in atoms which are incorporated into solids and are vibrating there at high temperatures.

As we saw in Chaps. 8 and 12, there are a number of interesting line shifts and splittings. In order to measure these exactly, the linewidth must be small compared to these shifts or splittings. Therefore, in Chap. 22 we shall discuss methods by which line broadening, and in particular Doppler broadening, can be avoided, thus permitting the experimenter to carry out Doppler-free spectroscopy. A simple method of reducing the Doppler broadening consists of cooling the source of the atomic beam which is being investigated. In order to reduce collisional broadening, one must ensure that the mean time between two collisions of one atom with other atoms is longer than the mean lifetime of the excited state. This is done by reducing the pressure in the experimental apparatus.

17. Many-Electron Atoms

17.1 The Spectrum of the Helium Atom

The simplest many-electron atom is the helium atom. In the ground state, its two *s* electrons exactly fill the innermost shell with the principal quantum number $n = 1$. There is no room for more electrons in this shell, as we shall see below.

In the excited state, one electron remains behind in the half-filled first shell, while the other is excited into a higher shell. Therefore we have

electron 1 in state $n = 1$ $l = 0$, and

electron 2 in state $n > 1$, $l = 0 \ldots n-1$.

In the previous chapters, we treated the spectra of atoms in which the quantum numbers of only *one* electron were sufficient to characterise the terms. Other electrons were either not present – as in the H atom – or they were all in so-called closed shells or closed subshells. That means, as we shall also see presently, that they make no contribution to the total angular momentum or magnetic moment of the atom.

The experimentally derived term scheme for helium (Fig. 17.1) is similar in some respects to those of the alkali atoms. It differs from them, however, in that there are two term systems which do not combine with each other, as if there were two kinds of helium atoms: a singlet and a triplet system. These names come from the fact that in the singlet system, all the terms are single, while in the triplet system, they are generally split into triplets.

What is important for practical applications, such as gas discharges and lasers, is that both the lowest state of the triplet system (2^3S in Fig. 17.1) and the second-lowest state of the singlet system (2^1S in Fig. 17.1) are metastable in the helium atom. "Metastable" means that the lifetime of the system is long compared to 10^{-8} s, which is the usual lifetime of a state which can be emptied by an allowed optical transition. An atom which is excited to one of these states can thus radiate its energy of about 20 eV only in a time that is long compared to 10^{-8} s.

Helium in the singlet state is also called parahelium. Unlike the alkali atoms, it has no fine structure. All its lines are single. The lowest term is given the symbol $1\,^1S$. Here the first 1 stands for the principal quantum number, the superscript 1 for the multiplicity (here singlet), and the letter S for the total orbital angular momentum, which in this case is zero. The higher terms are $2\,^1S$, $2\,^1P$, $3\,^1S$, $3\,^1P$, $3\,^1D$, etc. From the lack of fine structure, one can conclude that the spins of the two electrons are antiparallel, and add vectorially to a total spin $S = 0$. The same holds for the magnetic moment, $\mu_S = 0$. Here the upper case letters indicate quantum states which result from the coupling of many (here 2) electrons.

Triplet helium, which in contrast to the singlet system has fine structure, is called orthohelium. Its lowest level is $2\,^3S$. Here the 2 stands for the excited electron with

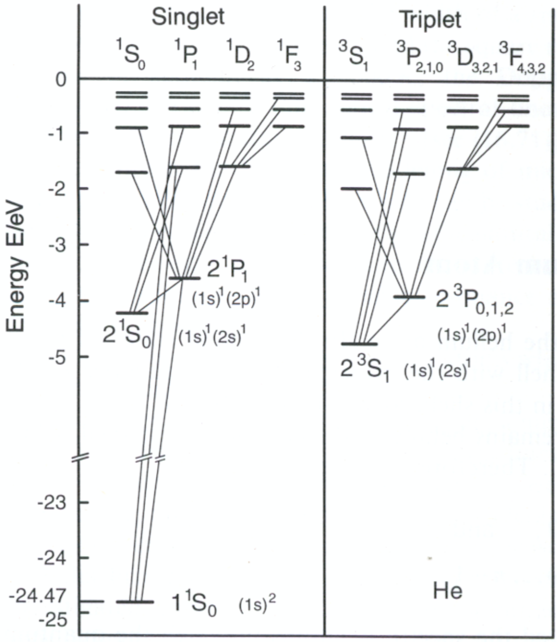

Fig. 17.1. Term scheme of the He atom. Some of the allowed transitions are indicated. There are two term systems, between which radiative transitions are forbidden. These are the singlet and triplet systems. The transitions in the singlet system span an energy range of 25 eV, while those in the triplet system span only 5 eV. The threefold splitting of the triplet terms (except for ^3S) due to spin-orbit coupling is not indicated here. The indices 0, 1, and 2 on the term symbol $^3P_{0,1,2}$ stand for the 3 possible quantum numbers $J = 0, 1, 2$

$n = 2$, the superscript 3 for the multiplicity (triplet), and the letter S for $L = 0$. Unfortunately, both the total spin quantum number and a term with the total orbital angular momentum $L = 0$ are represented by the same letter, S. The reader must be aware of this difference.

In this system, the spins of the two electrons are parallel to each other. The quantum number of the total spin is $s_1 + s_2 = S = 1$. The magnetic moment $\boldsymbol{\mu}_S = \boldsymbol{\mu}_{s_1} + \boldsymbol{\mu}_{s_2}$ is different from zero. The resulting total spin has three possible orientations with respect to an internal magnetic field $\boldsymbol{B}_l$ which is coupled to the orbital angular momentum of the electrons. The spin-orbit coupling resulting from this leads to a triple fine structure splitting of the terms which have non-vanishing total orbital angular momentum.

The spectrum of parahelium lies mostly in the ultraviolet, while that of orthohelium is in the infrared and visible. Combinations between the systems are not observed, i.e. there are no optical transitions between the singlet and triplet systems. If one compares corresponding configurations in the two non-combining systems, one discovers considerable differences in energy, especially for the low quantum numbers. The $2\,^1S_0$ state lies about 0.8 eV above the $2\,^3S_1$, and the $2\,^1P_1$ state about 0.25 eV higher than the $2\,^3P_2$ (the notation in this sentence is explained in Sect. 17.3.2). This energy difference between the singlet and triplet configurations is a result of the differences in the electrostatic interactions of the two electrons in parallel and antiparallel spin orientations. It is also called the symmetry energy, because it arises from the difference in the average distance between two electrons with symmetrical and antisymmetrical wavefunctions (see Sect. 17.2). For P states, this can also be seen in Fig. 17.9. More information about the theory will be given in Chap. 24, "the quantum theory of chemical bonding"; in particular, see Fig. 24.7.

17.2 Electron Repulsion and the Pauli Principle

Compared to the one-electron atom, the new factor in the helium atom is the repulsive interaction of the two electrons. For the total binding energy of the He atom, one must therefore write

$$E = -\underbrace{\frac{Ze^2}{4\pi\varepsilon_0 r_1}}_{\substack{\text{Nucleus –}\\ \text{electron 1}\\ \text{attrac-}\\ \text{tion at}\\ \text{distance}\\ r_1}} - \underbrace{\frac{Ze^2}{4\pi\varepsilon_0 r_2}}_{\substack{\text{Nucleus –}\\ \text{electron 2}\\ \text{attrac-}\\ \text{tion at}\\ \text{distance}\\ r_2}} + \underbrace{\frac{e^2}{4\pi\varepsilon_0 r_{12}}}_{\substack{\text{Electron 1 –}\\ \text{electron 2}\\ \text{repulsion}\\ \text{at mutual}\\ \text{distance}\\ r_{12}}} . \tag{17.1}$$

The repulsion energy of the two electrons naturally depends on the n, l states they occupy, because the spatial distribution of the electrons depends on the quantum numbers. This repulsion energy thus lifts the l degeneracy to a considerable degree.

The Schrödinger equation of this relatively simple two-electron problem cannot be solved exactly. The potential no longer has spherical symmetry and a separation into radial and angular parts is no longer possible. As a first approximation, in the independent-particle model, one neglects the third term and sets the total energy equal to the sum of two H-atom terms. The binding energy is then

$$E = -\left(\frac{RhcZ^2}{n^2}\right)_1 - \left(\frac{RhcZ^2}{n^2}\right)_2 \tag{17.2}$$

where the indices 1 and 2 refer to the two electrons. One would then expect the energy of the ground state to be

$$E_{\text{He}} = 2 \cdot (-54.4)\,\text{eV} = -108.8\,\text{eV} .$$

The experimental value is distinctly different from this. The total work of removing both electrons is 79 eV, 24.6 eV for removing the first electron (ionisation of the He to the singly charged positive ion He^+) and 54.4 eV for the removal of the second electron (ionisation of the singly charged He^+ to the doubly charged positive ion He^{2+}). The second value is the same as one would expect from a comparison with the hydrogen atom. There the ionisation energy is 13.6 eV. For helium, one would expect the energy to be four times as great, because the nucleus is doubly charged. The work of removing the first electron, however, is much smaller. The model for the binding energy must therefore be refined by taking into account the energy of the interaction of the two electrons. We shall present an approximation process in Sect. 19.4.

The observation that the helium atom has a $1\,^1S$ state but not a $1\,^3S$ state was the starting point for the Pauli principle (*Pauli* 1925). In its simplest form, it says:

> *The electronic states of an atom can only be occupied in such a way that no two electrons have exactly the same set of quantum numbers.*

The electrons must therefore differ in at least one quantum number. In addition to the orbital quantum numbers n, l and m_l, the spin quantum number s or m_s is taken into account here. An atomic state with a certain set of spatial quantum numbers (n, l, m_l) can thus be occupied by at most two electrons. Their spin (projection) quantum numbers $m_s = \pm 1/2$ must be different. In the 1^3S configuration, both electrons would have exactly the same quantum numbers, as we shall show in detail below. For more details see Sect. 19.4.

This principle is the generalisation of the previously stated empirical rule for all atoms with more than one electron: There is always a unique ground state which has the lowest principal quantum number. It has the highest multiplicity which is compatible with the principal quantum number. We discuss this point further in Sect. 19.3.

17.3 Angular Momentum Coupling

17.3.1 Coupling Mechanism

We have already learned that in the one-electron system, the individual angular momenta $\boldsymbol{l}$ and $\boldsymbol{s}$ combine to give a resultant angular momentum $\boldsymbol{j}$. There is a similar coupling between the angular momenta of different electrons in the same atom. We have already inferred, as an important result of empirical spectral analysis, that the total angular momentum of filled shells is equal to zero. This follows directly from the observation that the ground state of all noble gas atoms is the $^1S_0$ state. In calculating the total angular momentum of an atom, it is therefore necessary to consider only the angular momenta of the valence electrons, i.e. the electrons in non-filled shells. These angular momenta are coupled by means of magnetic and electric interactions between the electrons in the atom. They combine according to specific quantum mechanical rules to produce the total angular momentum $\boldsymbol{J}$ of the atom. These quantum rules are those which have already been discussed. The vector model provides insight into the composition of the angular momentum. There are two limiting cases in angular momentum coupling: the *LS* or Russell-Saunders coupling, and *jj* coupling.

17.3.2 *LS* Coupling (Russell-Saunders Coupling)

If the interactions $(\boldsymbol{s}_i \cdot \boldsymbol{l}_i)$ between the spin and orbital angular momenta of the individual electrons i are smaller than the mutual interactions of the orbital or spin angular momenta of different electrons [coupling $(\boldsymbol{l}_i \cdot \boldsymbol{l}_j)$ or $(\boldsymbol{s}_i \cdot \boldsymbol{s}_j)$], the orbital angular momenta $\boldsymbol{l}_i$ combine vectorially to a total orbital angular momentum $\boldsymbol{L}$, and the spins combine to a total spin $\boldsymbol{S}$. $\boldsymbol{L}$ couples with $\boldsymbol{S}$ to form the total angular momentum $\boldsymbol{J}$; cf. Fig. 13.11.

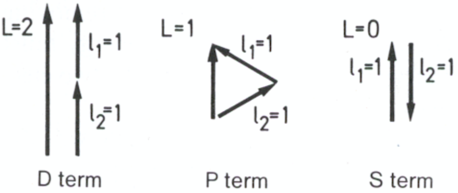

Fig. 17.2. Coupling of the orbital angular momenta of two electrons $\boldsymbol{l}_1$ and $\boldsymbol{l}_2$ to the total angular momentum $\boldsymbol{L}$. Coupling to *D*, *P* and *S*, corresponding to $L = 2$, 1, and 0. The picture is schematic. Exact addition of the angular momenta is accomplished as shown in Fig. 12.16

For a two-electron system like the He atom, the resulting behaviour is shown in Fig. 17.2. The orbital angular momentum $\boldsymbol{L}$ of the atom is the sum of the two electron orbital angular momenta

$$\boldsymbol{L} = \boldsymbol{l}_1 + \boldsymbol{l}_2 . \tag{17.3}$$

For the absolute value of L it again holds that $|\boldsymbol{L}| = \sqrt{L(L+1)}\,\hbar$ with the quantum number L, for which the following values are possible:

$$L = l_1 + l_2,\ l_1 + l_2 - 1 \ldots l_1 - l_2\,, \qquad \text{where} \qquad l_1 \geqq l_2\,.$$

The quantum number L determines the term characteristics:

$$L = 0, 1, 2 \ldots \text{indicates } S, P, D \ldots \text{terms}\,.$$

It should be noted here that a term with $L = 1$ is called a P term but this does not necessarily mean that in this configuration one of the electrons is individually in a p state.

For optical transitions the following selection rules hold:

$$\Delta l = \pm 1 \qquad \text{for the single electron}\,,$$

$$\Delta L = 0, \pm 1 \qquad \text{for the total system}\,.$$

$\Delta L = 0$ means here that the quantum states of two electrons change simultaneously, and in opposite directions. This is only possible when the coupling is strong, which is the case in heavy atoms.

Furthermore, for the total spin,

$$\boldsymbol{S} = \boldsymbol{s}_1 + \boldsymbol{s}_2 \qquad \text{with} \qquad |\boldsymbol{S}| = \sqrt{S(S+1)}\,\hbar\,. \tag{17.4}$$

The total spin quantum numbers S can take one of two values here, either

$$S = 1/2 + 1/2 \qquad \text{or} \qquad S = 1/2 - 1/2\,, \qquad \text{i.e.} \qquad S = 0 \qquad \text{or} \qquad S = 1\,.$$

The selection rule for optical dipole radiation is $\Delta S = 0$. This means that combinations between states with different total spins are not allowed, or in other words, that spin flipping is not associated with optical dipole radiation.

Finally, the interaction between $\boldsymbol{S}$ (or its associated magnetic moment $\boldsymbol{\mu}_S$), and the magnetic field $\boldsymbol{B}_L$, which arises from the total orbital angular momentum $\boldsymbol{L}$, results in a coupling of the two angular momenta $\boldsymbol{L}$ and $\boldsymbol{S}$ to the total angular momentum $\boldsymbol{J}$:

$$\boldsymbol{J} = \boldsymbol{L} + \boldsymbol{S}\,, \qquad |\boldsymbol{J}| = \sqrt{J(J+1)}\,\hbar\,. \tag{17.5}$$

The quantum number J can have the following values:

for $\quad S = 0\,, \quad J = L\,,$

for $\quad S = 1\,, \quad J = L+1, L, L-1\,,$

in which case all terms are triplets.

The individual angular momenta are combined according to exactly the same quantum rules with which we became acquainted in Chap. 13.

In the general case of a several-electron system, there are $2S+1$ possible orientations of S with respect to L, i.e. the multiplicity of the terms is $2S+1$ (if $S < L$). As an example, Fig. 17.3 shows the possible couplings in the case of $S = 1$, $L = 2$.

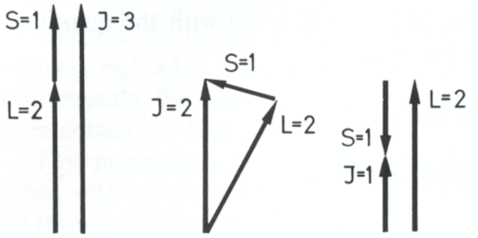

Fig. 17.3. Combination of spin (S) and orbital (L) angular momenta to form the total (J) angular momentum. If $L=2$ and $S=1$, J can assume the values 3, 2, or 1. This is a schematic representation. Figure 12.16 explains the method of exact addition of the angular momenta in the vector model

Using the helium atom as an example, we shall show once more which atomic terms can be derived from the given electron configurations. The lowest states of the helium atom have the following term symbols and quantum numbers:

- If both electrons are in the lowest shell, the electron configuration is $1s\ 1s$, or in the common notation $1s^2$. They then have the following quantum numbers:

  $$n_1 = n_2 = 1\,, \quad l_1 = l_2 = 0\,, \quad s_1 = 1/2\,, \quad s_2 = 1/2\,.$$

  The resulting quantum numbers for the atom are then either

  $$L = 0\,, \quad S = 0 \quad \text{for} \quad m_{s_1} = -m_{s_2}\,, \quad J = 0\,,$$

  the singlet ground state $^1S_0$; or

  $$L = 0\,, \quad S = 1 \quad \text{for} \quad m_{s_1} = m_{s_2}\,, \quad J = 1\,,$$

  the triplet ground state $^3S_1$. Only the singlet ground state is actually observed. The triplet ground state is forbidden by the Pauli Principle, because in it the two electrons would not only have the same quantum numbers n and l, but they would also have the same spin orientation m_s.

- However, when one electron remains in the shell with $n=1$, while the other is raised into the state with $n=2$, that is in the electron configuration $1s\,2s$, we have the following quantum numbers:

  $$n_1 = 1\,, \quad n_2 = 2\,, \quad l_1 = l_2 = 0\,, \quad s_1 = 1/2\,, \quad s_2 = 1/2\,.$$

  This yields either $L=0$, $S=0$, $J=0$, the singlet state $^1S_0$; or $L=0$, $S=1$, $J=1$, the triplet state $^3S_1$. Both states are allowed and are observed.

- In the same way, the states and term symbols can be derived for all electron configurations. More on this subject is to be found in Sect. 19.1.

We finally arrive at the term scheme with the allowed optical transitions by taking into account the selection rules. Intercombination lines with $\Delta S = 1$ are forbidden, because there is no spin flipping with optical dipole radiation. This is the reason for the existence of non-combining term systems like that in Fig. 17.1.

The complete nomenclature for terms or energy states of atoms, which we have already used, is then

$$n^{2S+1}L_J\,.$$

One first writes the principal quantum number n of the most highly excited electron, which is called the *valence* electron. The superscript is the multiplicity $2S+1$. It is followed by the alphabetical symbol S, P, D... for the total orbital angular momentum L; the subscript to this symbol is the quantum number J for the total angular momentum of the atom.

For many-electron systems, this must be expanded over the possible multiplicities as shown below:

For two electrons	$S=0$ Singlet	$S=1$ Triplet		
For three electrons	$S=1/2$ Doublet	$S=3/2$ Quartet		
For four electrons	$S=0$ Singlet	$S=1$ Triplet	$S=2$ Quintet	
For five electrons	$S=1/2$ Doublet	$S=3/2$ Quartet	$S=5/2$ Sextet	etc.

According to the rules for coupling of angular momenta, which have been treated in this section, the possible atomic states can now be easily derived from known electron configurations. We shall only explain a simple example here. In the configuration

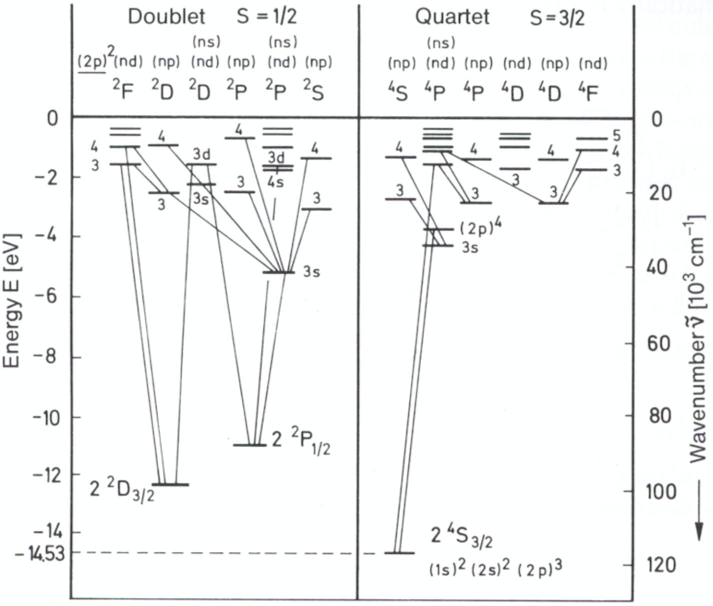

Fig. 17.4. Term diagram for the nitrogen atom (only simple terms, no J splitting). Nitrogen as a doublet and a quartet system. The electronic configuration of the valence electrons is given at the top

Fig. 17.5. Term diagram for the carbon atom (only simple terms, no J splitting). Carbon has a singlet and a triplet system. The configuration of the valence electrons is given at the top ▸

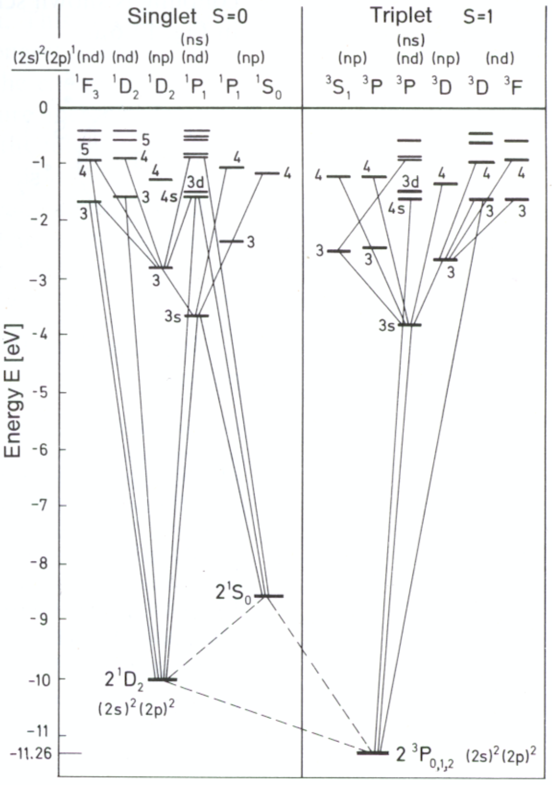

ns n's, i.e. with two non-equivalent *s* electrons, the total orbital momentum is necessarily $L = 0$, because $l_1 = l_2 = 0$. The spins of the two electrons can be either parallel or antiparallel. This means that the total spin quantum number $S = 1$ or $S = 0$. In either case, the total angular momentum $J = S$. The possible terms of the configuration *ns n's* are therefore the triplet term $^3S_1$ and the singlet term $^1S_0$.

We shall discuss other examples in Chap. 19, when we know somewhat more about the energetic order of these possible terms.

To make the above somewhat more clear, Figs. 17.4 and 17.5 show the Grotrian diagrams for the nitrogen and carbon atoms. Here, only those terms are taken into account which result from the excitation of a single electron, the so-called valence electron. Of the remaining electrons, only those need be considered which are in non-closed subshells. The remaining electrons form the spherically symmetric core of the electronic shell. The terms and term symbols resulting from *LS* coupling and from the quantum states of the individual electrons can now be immediately understood, and can be derived from the electron configuration, which is also given. We shall return to these many-electron atoms in Chap. 19.

17.3.3 *jj* Coupling

The second limiting case for coupling of electron spin and orbital angular momenta is the so-called *jj* coupling, which occurs only in heavy atoms, because the spin-orbit coupling for each individual electron increases rapidly with the nuclear charge *Z*.

In *jj* coupling, the spin-orbit interaction $(\boldsymbol{l}_i \cdot \boldsymbol{s}_i)$ for a single electron is large compared to the interactions $(\boldsymbol{l}_i \cdot \boldsymbol{l}_j)$ and $(\boldsymbol{s}_i \cdot \boldsymbol{s}_j)$ between different electrons. This type of coupling is shown schematically in Fig. 17.6b. For comparison, *LS* coupling is shown in Fig. 17.6a.

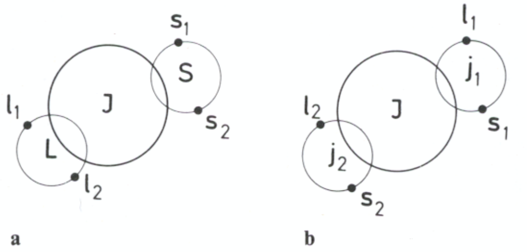

Fig. 17.6. a) Schematic representation of *LS* coupling between two electrons. **b)** *jj* coupling between two electrons. In *jj* coupling, the angular momenta ***L*** and ***S*** are not even defined

In *jj* coupling, the angular momenta of individual electrons couple according to the pattern

$$\boldsymbol{l}_1 + \boldsymbol{s}_1 \rightarrow \boldsymbol{j}_1 , \quad \boldsymbol{l}_2 + \boldsymbol{s}_2 \rightarrow \boldsymbol{j}_2 ,$$

and so on to give individual total angular momenta $\boldsymbol{j}$. These then combine vectorially to give the total angular momentum $\boldsymbol{J}$ of the atom. Here $\boldsymbol{J} = \Sigma \boldsymbol{j}_i$ and

$$|\boldsymbol{J}| = \sqrt{J(J+1)}\,\hbar .$$

In this type of coupling, the quantum number *J* arises from a generalised quantum mechanical vector model. A resultant orbital angular momentum ***L*** is not defined. There are therefore no term symbols *S, P, D*, etc. One has to use the term notation (j_1, j_2) etc., where *j* are the angular momentum quantum numbers of the individual electrons. It can easily be shown that the number of possible states and the *J* values are the same as in *LS* coupling.

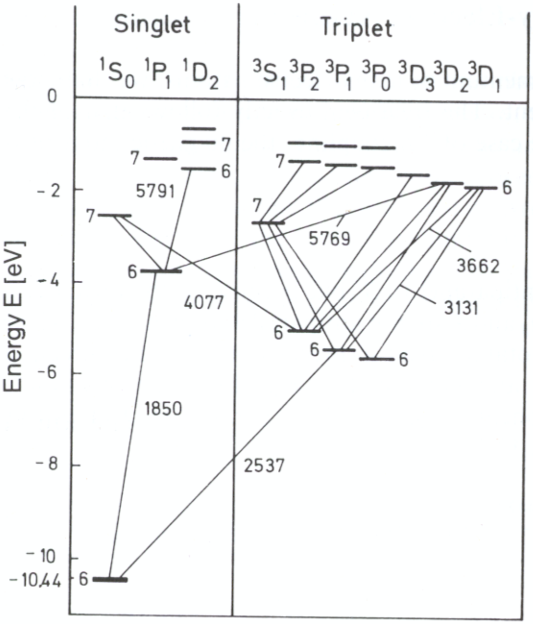

◀ **Fig. 17.7.** Simplified energy diagram of the mercury atom as an example of a heavy atom with term symbols corresponding to *LS*-coupling. The wavelengths [Å] of a few of the more important lines are given. The strongest line in the spectrum of a mercury lamp is the line at 2537 Å which results from the intercombination of the 6^1S_0 and the 6^3P_1 states. Intercombination between terms of different multiplicity is strictly forbidden in light atoms. In heavy atoms it is possible. This line corresponds to the energy loss of 4.9 eV in the Franck-Hertz experiment, Sect. 8.8

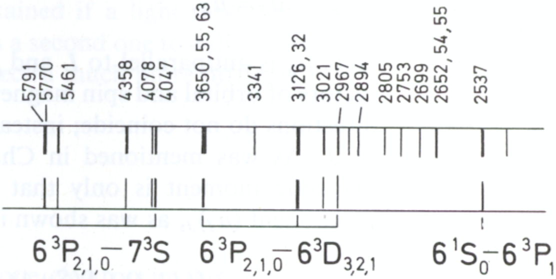

Fig. 17.8. Photographically recorded spectrum of a low-pressure mercury lamp: segment between 2500 and 5800 Å. Due to the superposition of the different series in the spectrum, which are shown in the energy diagram Fig. 17.7, a series structure cannot be *immediately* recognised in the spectrum of a heavy, several-electron atom, as might be inferred from the energy diagram

Purely *jj* coupling is only found in *very* heavy atoms. In most cases there are intermediate forms of coupling, in such a way, for example, that the intercombination between terms of different multiplicity is not so strictly forbidden. This is called intermediary coupling. The most prominent example of this is the strongest line in the spectrum of mercury high-pressure lamps, $\lambda = 253.7$ nm (compare the energy diagram in Fig. 17.7 and the photograph of the spectrum of a low-pressure mercury lamp in Fig. 17.8). In the frequently used high-pressure mercury lamps, the intensity distribution of the spectrum is different from that of a low-pressure lamp. The 253.7 nm line is relatively most strongly emitted, in addition broadened, and reabsorbed. This is an intercombination line between the singlet and triplet systems. The selection rule for optical transitions is $\Delta J = 0, \pm 1$, and a transition from $J = 0$ to $J = 0$ is forbidden. An example for the transition from *LS* to *jj* coupling is shown in Fig. 17.9.

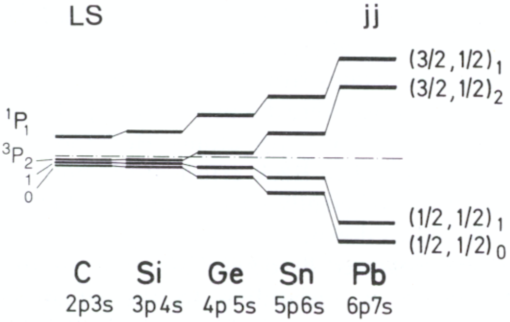

Fig. 17.9. Transition from *LS* coupling in light atoms to *jj* coupling in heavy atoms in the series C – Si – Ge – Sn – Pb. In carbon the $^3P_0 - {}^3P_1$ and $^3P_1 - {}^3P_2$ distance are 20 and 40 cm^{-1}, while the $^1P_1 - {}^3P_2$ distance is 1589 cm^{-1}. The term nomenclature is that of *LS* coupling for carbon, and of *jj* coupling for lead. The quantum symbols of the two outermost electrons are given. The symbol $(3/2, 1/2)_1$ means $j_1 = 3/2$, $j_2 = 1/2$, $J = 1$

17.4 Magnetic Moments of Many-Electron Atoms

Having calculated the total angular momentum of many-electron atoms, we shall now also calculate the total magnetic moment. The treatment exactly follows that of the one-electron system in Chap. 13. In the case of LS coupling, the magnetic moment is composed of

$$\boldsymbol{\mu}_L + \boldsymbol{\mu}_S = \boldsymbol{\mu}_J\,.$$

Here $\boldsymbol{\mu}_L$ is antiparallel to $\boldsymbol{L}$ and $\boldsymbol{\mu}_S$ is antiparallel to $\boldsymbol{S}$, but because of the different g factors of orbital and spin magnetism, $\boldsymbol{\mu}_J$ and $\boldsymbol{J}$ are not antiparallel to each other. Their directions do not coincide; instead the total moment $\boldsymbol{\mu}_J$ precesses around the direction of $\boldsymbol{J}$. As was mentioned in Chap. 13 and illustrated in Fig. 13.9, the observable magnetic moment is only that component of $\boldsymbol{\mu}_J$ which is parallel to $\boldsymbol{J}$. For this component $(\boldsymbol{\mu}_J)_J$, as was shown in Sect. 13.5,

$$|(\boldsymbol{\mu}_J)_J| = \frac{3J(J+1)+S(S+1)-L(L+1)}{2\sqrt{J(J+1)}}\cdot \mu_\mathrm{B} = g_J\sqrt{J(J+1)}\,\mu_\mathrm{B} \tag{17.6}$$

with the Landé factor

$$g_J = 1 + \frac{J(J+1)+S(S+1)-L(L+1)}{2J(J+1)}\,. \tag{17.7}$$

In one chosen direction z, the only possible orientations are quantised and they are described by whole or half-integral values of the quantum number m_J, depending on the magnitude of J.

$$(\boldsymbol{\mu}_J)_{J,z} = -m_J g_J \mu_\mathrm{B} \tag{17.8}$$

with

$$m_J = J, J-1, \ldots -J\,.$$

The contents of this chapter are the quintessence of years of spectroscopic work: measurement of spectra, setting up of term schemes, determination of quantum numbers, and so on. Measurements in magnetic fields have also been an essential tool. If one applies the insights discussed in Chap. 13 to many-electron atoms, one can determine the magnetic quantum numbers of the atomic states from measurements of the splitting of spectral lines. The same considerations which were discussed in Chap. 13 on the behaviour of atoms in magnetic fields apply to many-electron atoms. Here too, the normal and anomalous Zeeman effects and the Paschen-Back effect are important limiting cases. The LS coupling can be broken in sufficiently strong magnetic fields, and in very strong fields, even the jj coupling breaks down.

The atomic magnetic moments can also be measured by determining the macroscopic material constant *magnetic permeability*, μ_r, according to the equation $B = \mu_\mathrm{r}\mu_0 H$ (H is the magnetic field strength). Details are given in H. Haken and H.C. Wolf, *Molecular Physics and Elements of Quantum Chemistry*, Sect. 3.6.

17.5 Multiple Excitations

Let it be only briefly mentioned here that observed spectra can be made much more complicated by multiple excitation processes, such as those in which several electrons are involved and change their states in the atom. This is especially likely in systems where there is strong mutual interaction between the electrons. In ionisation processes, for example, it is possible that a second electron is simultaneously excited. Excitation energies higher than the ionisation limit can be obtained if a light quantum simultaneously removes one electron (ionisation) and raises a second one to a discrete excitation level. This makes the analysis of heavy-atom spectra much more difficult.

Problems

17.1 The energy levels of helium-like atoms with one electron in the ground state ($n = 1$) and the other in an excited state ($n > 1$) can be expressed as

$$E = -RhcZ^2 - \frac{Rhc(Z-1)^2}{n^2}.$$

This expression is based on the assumption that the ground state electron completely shields one unit of nuclear charge. Discuss the plausibility of the expression. Calculate the energy levels for helium with $n = 2$, 3 and 4 and compare them with the experimental results. Why does the accuracy of the above expression for E increase as n increases?

17.2 Show that the sum $\sum(2J+1)$ over all possible values of J for a given pair of quantum numbers L and S is equal to the product $(2L+1)(2S+1)$. What is the physical meaning of this product?

17.3 Discuss a two-electron system with a $2p$ and a $3d$ electron for the case of jj coupling and show that the number of possible states and their total angular momentum J are the same as in LS coupling.

17.4 a) Ignoring spin-orbit coupling, determine the number of possible terms of an excited carbon atom with the electronic configuration $1s^2 2s^2 2p\,3d$.

b) Calculate the effective magnetic moment of an atom in the ground state with the configuration $1s^2 2s^2 2p^6 3s^2 4s^2 3d^3$, assuming that L has the largest possible value consistent with Hund's rule (Sect. 19.2) and the Pauli principle.

c) Calculate the ground state of the atoms with the electronic configurations $4d\,5s^2$ (Y) or $4d^2 5s^2$ (Zr). [The closed shells are not given. L is determined as under b).]

d) The manganese atom ($Z = 25$) has in its ground state a subshell which is exactly half-filled with 5 electrons. Give the electronic configuration and the ground state of the atom.

17.5 a) Calculate the maximum components of the magnetic moments in the direction of the magnetic field for vanadium (^4F), manganese (^6S) and iron (^5D), if beams of these atoms are split into 4, 6 or 9 parts in a Stern-Gerlach experiment.

b) What is the term symbol of the singlet state with a total splitting of $\bar{\nu} = 1.4\ \mathrm{cm}^{-1}$ in a magnetic field $B_0 = 0.5$ tesla?

18. X-Ray Spectra, Internal Shells

18.1 Introductory Remarks

Up to this point, the discussion has been concerned with the energy states and spectra of the most weakly bound electrons. In the lighter atoms, these are usually the outermost or valence electrons. If we now turn to x-ray spectra, we shall be concerned with the energy states of electrons in inner shells. We shall see, however, that x-ray spectra can for the most part be treated as one-electron spectra, although they belong to many-electron atoms.

Historically, it was the x-ray spectra which led to the theory of the shell structure of the atom (*Kossel* 1914). At present, however, we shall assume that the shell structure is familiar as we turn to the x-ray spectra.

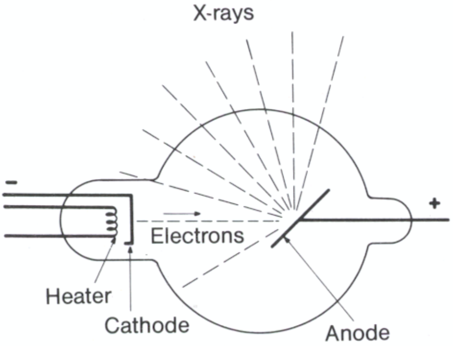

Fig. 18.1. An x-ray tube, schematically

X-rays are usually generated by irradiating an anode, which is often called the anticathode, with fast electrons (Fig. 18.1). We point out here that x-rays may also be produced by electron impact or collisional excitation of free atoms, and thus independently of solid-state influences. The x-rays are detected by photographic plates, film, counting tubes, or more recently, by semiconductor detectors. The latter are made as silicon or germanium diodes. Absorption of x-rays in the "space-charge" zone releases charge carriers. These can be measured as in an ionisation chamber. Pulse-height analysis permits the apparatus to be used both to measure the energy of the x-ray quanta and as a simple spectrometer. For higher resolution spectroscopy and wavelength measurements, one still uses the crystal spectrometer described in Sect. 2.4.5. One can also obtain a rough estimate of the wavelength of x-rays by measuring their "hardness" – their ability to penetrate solids.

18.2 X-Radiation from Outer Shells

By "x-rays", we usually mean electromagnetic radiation (light) which has a wavelength shorter than that of ultraviolet light – though there is no sharp boundary. The range is usually considered to be 0.1 to 10 Å, which corresponds to quantum energies of 1 – 100 keV. The x-ray region is attained according to the series formula (Sect. 8.2)

$$\bar{\nu} = RZ^2(1/n^2 - 1/n'^2)$$

for hydrogen-like atoms, i.e. atoms with only one electron, if the nuclear charge is large enough. For $Z = 20$, the quantum energies are already 400 times as large as the energies of corresponding transitions in the hydrogen atom with $Z = 1$. It is generally not possible to generate such "Balmer series" for highly ionised atoms in the laboratory, but these spectra can be observed in stellar atmospheres. Recently, such experiments have also become feasible through the use of particle accelerators; cf. Sect. 8.6. The Balmer series of U^{91+} was observed in the spectral range from 15 to 35 keV, and the Lyman series near 100 keV.

18.3 X-Ray Bremsstrahlung Spectra

If an anticathode is bombarded with electrons which have passed through an accelerating voltage V_0, x-rays are generated. Spectral analysis of these reveals that

- there is always a continuum, the *x-ray bremsstrahlung* (Fig. 18.2),
- and under certain conditions, there is in addition a line spectrum, the *characteristic spectrum* (Fig. 18.3).

If the intensity is plotted against the frequency, see Fig. 18.4, rather than the wavelength (as in Fig. 18.2), and if care is taken to ensure that the intensity distribution of the x-ray spectrum is not modified by reabsorption in the anticathode (cf. Sect. 18.6), the bremsstrahlung spectrum for an accelerating voltage V_0 is described, to a good approximation (outside the low-energy range) by

$$I(\nu) = \text{const} \cdot Z(\nu_{\max} - \nu) , \qquad (18.1)$$

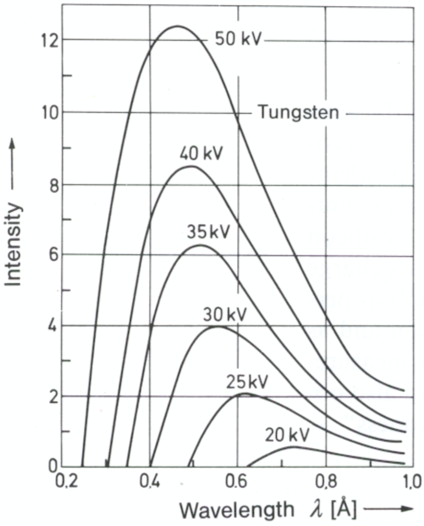

Fig. 18.2. X-ray bremsstrahlung. Spectral energy distribution of the x-rays emitted from a massive tungsten anticathode at various accelerating voltages for the bombarding electrons. The intensity is given in arbitrary units

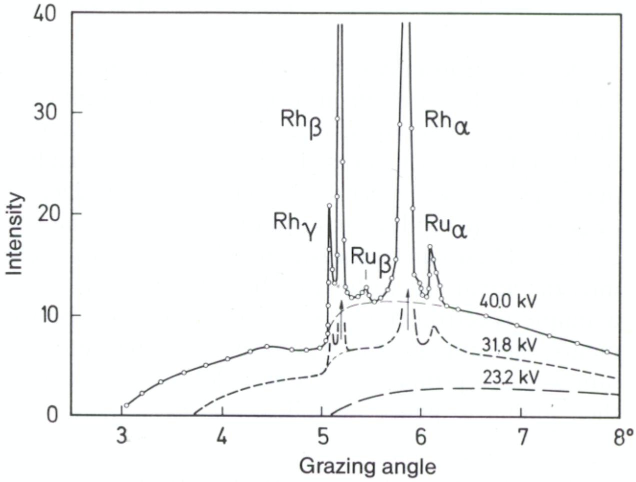

Fig. 18.3. Line spectrum of a Rh anticathode doped with Ru impurity. The lines are superimposed on the bremsstrahlung spectrum. The intensity is plotted against the grazing angle of the crystal spectrometer instead of the wavelength

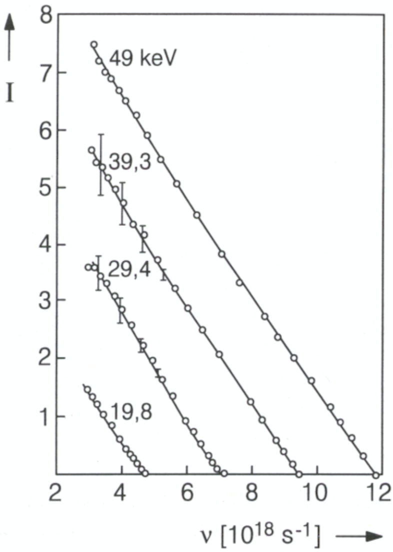

◄ **Fig. 18.4.** The intensity I in the x-ray bremsstrahlung spectrum as a function of the frequency for different primary energies of the electrons used for excitation. The measurement was carried out with a thick anticathode (after Kulenkampf)

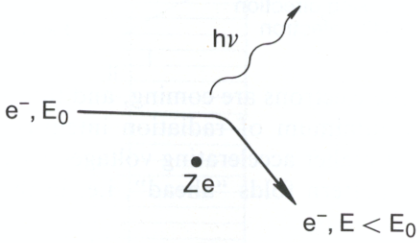

Fig. 18.5. Origin of x-ray bremsstrahlung. An electron with energy E_0 is deflected in the field of a nucleus and slowed down. In the process a quantum of light is emitted

where I is the intensity of the radiation (energy per time and frequency interval and solid angle) and Z is the atomic number of the anticathode material. The limiting frequency $\nu_{\max}$ is given by

$$h\nu_{\max} = e \cdot V_0 \, . \tag{18.2}$$

This means that the high-energy or short-wavelength limit of the x-ray spectrum $\nu_{\max}$ is given by the energy equivalent eV_0. The bremsstrahlung spectrum is a result of the fact that when electrons pass close to the atomic nuclei, they are deflected and slowed down (Fig. 18.5). A positive or negative accelerated charge will, according to classical electrodynamics, emit electromagnetic radiation. This is "white" or continuous x-ray bremsstrahlung. In terms of quantum theory, this can be understood as follows: for each braking incident, a quantum of light $h\nu = E_0 - E$ is emitted. However, since the beginning and end states are not quantised – the electrons are free, not bound – a "white" spectrum arises when there are many individual events.

The reaction equation is

$$\text{Atom} + e^-(\text{fast}) \rightarrow \text{Atom} + e^-(\text{slow}) + h\nu \, .$$

In the limiting case, the entire energy of the electron is emitted in a single quantum in the course of a single braking event. This x-ray quantum then has the energy $h\nu_{\max} = eV_0$. The measurement of this short-wave limit is one method of determining Planck's constant h with great precision. However, one must be careful about such precision measurements, because the work of escaping the solid, and the band structure of the solid, lead to uncertainties or corrections of a few electron volts in the energies at the short-wavelength limit of the bremsstrahlung spectrum. The bremsstrahlung spectrum thus gives very little information about atomic structure.

The spatial distribution of the radiation can also be explained in terms of the classical view of bremsstrahlung. With a thin anticathode, in which multiple events are less probable, and with energies eV_0 which are not too high, the distribution is the same as with the classical Hertzian dipole. The maximum is perpendicular to the direction

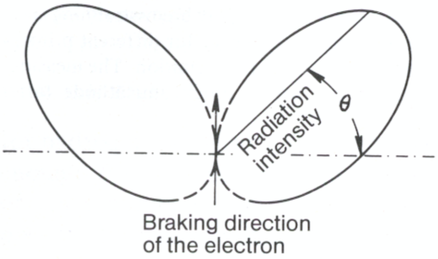

Fig. 18.6. Spatial distribution of the bremsstrahlung

from which the electrons are coming, and thus to the direction in which braking is occurring. The minimum of radiation intensity is in the direction of electron travel (Fig. 18.6). At higher accelerating voltages V_0 a relativistic calculation is required and the radiation pattern folds "ahead", i.e. in the beam direction.

18.4 Emission Line Spectra: Characteristic Radiation

Characteristic radiation consists of a relatively small number of lines. Figure 18.3 gives an example of this. The lines are again grouped into series, which converge to a short-wavelength limit, which is called an "edge". With a rhodium anticathode, for example, one can observe the following lines and series by increasing the accelerating voltage on the electrons in steps:

For accelerating voltages $V_0 > 0.5$ kV, the lines of the *M* series,
For accelerating voltages $V_0 > 3.0$ kV, the *L* series also,
For accelerating voltages $V_0 > 23$ kV, the *K* series as well.

The lines of the *K* series are doublets.

In general it holds for characteristic spectra that while optical spectra contain a large number of lines which depend on the nuclear charge *Z* in a rather complicated way, and which are strongly influenced by chemical bonding, x-ray spectra include a limited number of lines which can be grouped into a few series. There is also a clear relationship to the nuclear charge (Fig. 18.7). Corresponding lines and edges are found at increasing quantum energies as the nuclear charge increases. The series are designated by the letters *K*, *L*, *M*, *N*, ... and the lines within the series by Greek lower case letters beginning with α. The fine structure splitting of the lines is indicated by numbers written as subscripts.

To a good approximation, the first line of the *K* series, the line K_α, can be described for atoms with different nuclear charge numbers *Z* by the expression

$$\bar{\nu}_{K_\alpha} = \tfrac{3}{4}R(Z-1)^2 \equiv R(Z-1)^2(1/1^2 - 1/2^2)\,. \tag{18.3}$$

The first lines of the *L* series (L_α) are described by

$$\bar{\nu}_{L_\alpha} = \tfrac{5}{36}R(Z-7.4)^2 \equiv R(Z-7.4)^2(1/2^2 - 1/3^2)\,. \tag{18.4}$$

A linear relationship between $\sqrt{\nu}$ and the nuclear charge number *Z* for analogous x-ray lines or edges (see Sect. 18.6) in the spectra of different elements was discovered in 1913 by *Moseley* (Moseley lines; see Fig. 18.8). Comparison with the Balmer formula for hydrogen suggests that for the *K* line the nuclear charge is screened by one unit of charge, while for the *L* line, it is screened by almost eight units.

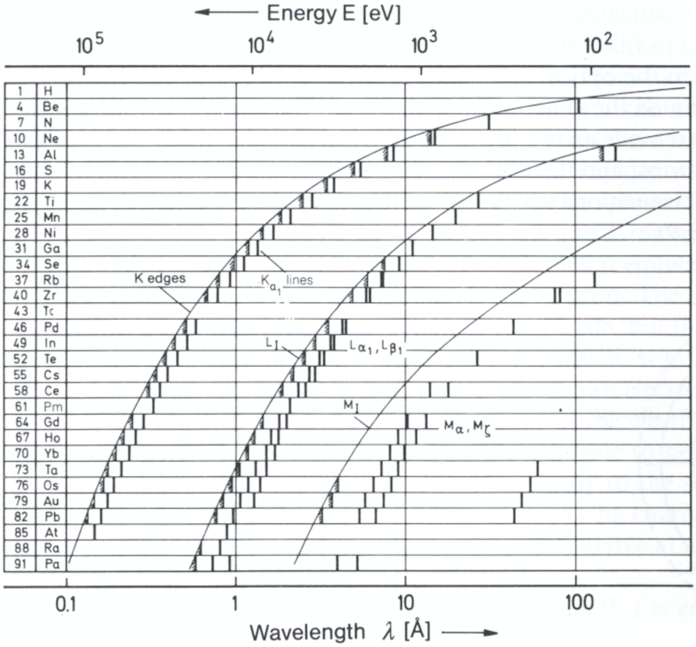

◀ **Fig. 18.7.** Spectral positions of the characteristic x-ray emission lines and the absorption edges of the elements. The quantum energies increase with increasing nuclear charge number

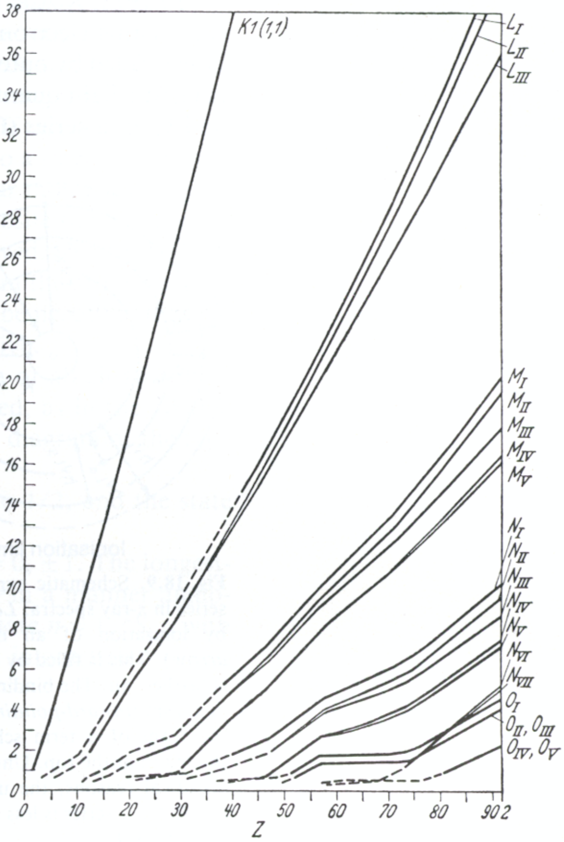

Fig. 18.8. Moseley diagram of the absorption edges. For the edge frequencies $\bar{\nu}$, $\sqrt{\bar{\nu}/R} = (Z-s)/n$, where s is the screening number (cf. (18.3), n and s are different for different shells, and this is why the observed Moseley lines are not parallel. The lines for the spin doublets, e.g. $L_{\mathrm{II,III}}$ diverge at the top because spin-orbit coupling increases with Z; cf. Sect. 18.5. [From K.H. Hellwege: *Einführung in die Physik der Atome*, Heidelberger Taschenbücher, Vol. 2, 4th ed. (Springer, Berlin, Heidelberg, New York 1974) Fig. 72] ►

Chemical bonding of an atom has only a slight influence on its x-ray spectrum. However, exact measurement of this effect does provide important information about the behaviour of electrons in chemical bonds. This is of importance in molecular and solid-state physics.

The emission of x-rays can be elicited not only by bombarding an anticathode with electrons, but also by irradiation of atoms, molecules or solids with x-rays. This is called x-ray fluorescence.

The wavelength of the x-radiation is greater than, or at least equal to, that of the exciting light, but other than that, it is independent of the wavelength of the exciting radiation within certain limits. The lines of a series appear in a fluorescence spectrum, and then all of them at once, only when the quantum energy of the exciting radiation is at least as great as the quantum energy of the highest-energy, or shortest-wavelength line in the characteristic spectrum. It is the same with excitation of x-radiation by electron bombardment: the kinetic energy of the elctrons eV_0 must be at least as great as the quantum energy of the shortest-wavelength line of the series before this series appears in the emission spectrum. Thus emission of the K_α line cannot be excited by the quantum energy of K_α; instead it is necessary to supply the energy of the K edge. This is the energy to which the lines of the K series converge, the series limit. From this and other observations, it was concluded that x-ray lines correspond to states of "inner" electrons which are bound in filled shells, in contrast to the more loosely bound outer electrons, which give rise to the optical spectra.

In 1916, *Kossel* interpreted the generation of the x-ray line spectra as follows: first the exciting electron must remove an atomic electron from an inner shell. The resulting hole is filled by outer electrons, and their binding energy is released in the form of characteristic light quanta. All transitions which end on the same inner shell occur together, and form a series (Fig. 18.9).

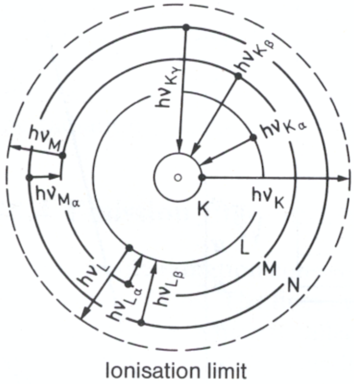

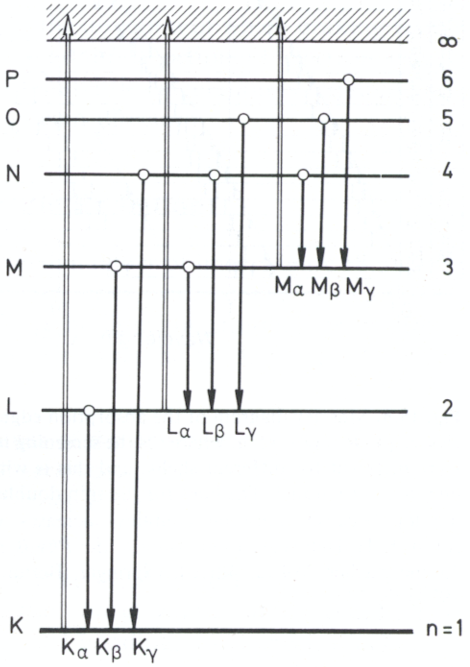

Fig. 18.9. Schematic explanation of the *K*, *L* and *M* series in x-ray spectra. *Left:* An electron hole is formed by ionisation of an inner shell (*outward-pointing arrow*). This is filled by an electron from a shell which is farther out. The binding energy is emitted as an x-ray quantum (*inward-pointing arrow*). *Right:* The same in the form of a term scheme. The ionisation limit is shaded in at the top. Unfortunately, in practice and by historical reasons, the use of the greek letters in the *L*, *M*, *N*... series is less systematic than indicated here, cf. Fig. 18.9

The quantitative observations described by (18.3) and (18.4) thus become understandable: the atomic number Z is screened by one elementary charge in the K shell and by $7.4\,e_0$ in the L shell for the electron making the transition.

The transitions involving inner shells are much more energetic than those in the outermost shell, because the nuclear charge is shielded only by those electrons in still lower shells. This results in screening to a charge $(Z-1)$ for the K_α lines, and to $(Z-7.4)$ for the L_α lines. The field strength in the interior of a sphere with a uniformly charged surface is zero, so the external electrons make no contribution to the field experienced by the inner ones.

18.5 Fine Structure of the X-Ray Spectra

The x-ray transitions indicated by Greek letters, K_α, K_β, L_α, L_β, etc. thus start from terms with different principal quantum numbers n. To understand the "fine structure" of x-ray spectra, that is the occurrence of several components in a given transition, one must also take into account the orbital angular momentum and spin of the electrons.

For electrons in inner shells, orbital degeneracy (l degeneracy) is naturally lifted. The reason for this, the different degrees of screening for electrons with different orbital angular momenta and the associated differences in the Coulomb potential, has already been discussed in the case of the spectra of alkali atoms (Sect. 11.2). Furthermore, we must also take into account the actual fine structure due to spin-orbit coupling. The energy of this coupling increases rapidly with nuclear charge, as Z^4 (Sect. 12.8). In heavy atoms such as uranium the spin-orbit splitting amounts to as much as 2 keV! One can understand the structure of x-ray spectra if one realises that a missing electron, or a hole, in an otherwise full shell is equivalent to a single electron in an otherwise empty shell or also to an added positron. The angular momentum of the remainder of the atom clearly has the same magnitude, but the opposite sign, compared to the angular momentum of the electron which was removed. Naturally this equivalence goes only as far as the sign: to remove an electron from the atom we must apply energy. If we consider the binding energy of the electron to be negative, then we must consider the energy required to generate a hole to be positive.

X-ray spectra can thus be understood, similarly to the spectra of alkali atoms, as one-electron (or one-hole) spectra. The terms may be characterised, as in the alkalis, by the quantum numbers of *one* electron; we thus arrive at a term diagram of the type shown in Fig. 18.10.

In the K shell, $n = 1$, l can have only the value 0, j is equal to 1/2, and the state is denoted by the symbol ${}^2S_{1/2}$.

For optical transition, the selection rules are $\Delta l = \pm 1$ and $\Delta j = 0, \pm 1$. The longest-wavelength lines of the K series, $K_{\alpha 1}$ and $K_{\alpha 2}$, are thus produced in a manner analogous to the two sodium D lines; see Sect. 12.9. They connect the state $n = 1$, ${}^2S_{1/2}$ with the states $n = 2$ ${}^2P_{1/2}$ and ${}^2P_{3/2}$, which are split by the spin-orbit interaction.

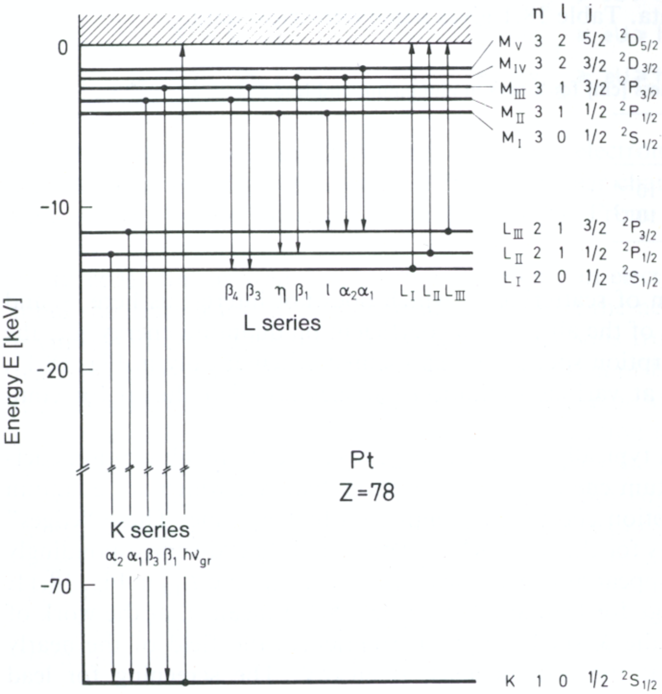

Fig. 18.10. Fine structure diagram for the x-ray spectra of a platinum anode with $Z = 78$. The notations for the series, the lines, and the quantum numbers are shown. Arrows pointing upwards mean absorption, those pointing downwards mean emission. The use of Greek letters to denote the individual lines is not systematic and is not uniform in the literature. – The spacings between the L subshells L_{I}, L_{II}, L_{III} and the M subshells $M_{\text{I}} - M_{\text{V}}$ are not shown to scale. For a given l-value, they result from the normal doublet splitting; otherwise, they are produced by differing screening of the nuclear charge and are therefore not all equal. The Greek-letter symbols for x-ray lines are of historical origin and are not identical to the systematic notation used in Fig. 18.9

Correspondingly, we can understand all of the fine structure of x-ray spectra. The shells which are characterised by the quantum numbers n are also split up into subshells. The latter are numbered using Roman numerals (e.g. L_{I}, L_{II}, L_{III} in Fig. 18.10). A subshell is characterised by a triplet of quantum numbers n, l, and j. The energy splitting between the edges L_{I}, L_{II}, and L_{III} has, as indicated in Fig. 18.10, a variety of origins. The spacing between L_{II} and L_{III}, i.e. between $^2P_{1/2}$ and $^2P_{3/2}$, is the well-known doublet splitting, which increases with the fourth power of the screened nuclear charge Z (cf. Sects. 12.8 and 18.4). The spacing between L_{I} and L_{II}, on the other hand, results from variations in screening. The latter is produced only by the inner electrons and is less dependent on Z. This is clarified in the Mosely diagram (Figs. 18.7 and 8).

If the atoms are not free, but instead are bound in a solid, then the upper occupied electronic energy levels are broadened into energy bands. X-ray lines resulting from transitions between the broad uppermost occupied energy band and an inner electronic level, which is not broadened by solid state effects, have a characteristic structure. Their width and intensity distribution can give a direct picture of the width of the uppermost energy band and its occupation by the electrons.

18.6 Absorption Spectra

X-rays, like any other electromagnetic radiation, are absorbed and scattered on passing through matter. The primary experimentally determined quantity is the extinction coefficient μ, defined by the equation $I = I_0 \exp(-\mu x)$, where x is the thickness of the material irradiated, I_0 is the incident intensity, and I is the transmitted intensity. The result of a measurement is often given as the half-absorption thickness, $d = \mu^{-1} \ln 2$. The half-absorption thickness depends, in general, on the material irradiated and on the energy of the x-ray quanta. Table 18.1 gives some numerical data.

Table 18.1. Half-absorption thickness [cm] for x-rays in aluminium and lead

V_0 [kV]	Al	Pb
10	$1.1 \cdot 10^{-2}$	$7.5 \cdot 10^{-4}$
100	1.6	$1.1 \cdot 10^{-2}$

The extinction is the sum of scattering – which does not interest us here – and absorption. The dependence of the absorption coefficient on quantum energy, i.e. the spectral distribution in absorption spectra, is represented schematically in Fig. 18.11, where the emission spectra at various excitation energies are also shown for comparison.

X-ray absorption spectra typically display a large decrease in the absorption coefficient with increasing quantum energy, and absorption "edges", which are quantum energies at which the absorption coefficient jumps to a higher value. These "edges" correspond to the series limits for the K, L, M, ... series, and they are correspondingly labelled. The subshells also appear as edges, for example L_{I}, L_{II}, and L_{III} in Fig. 18.11.

The position of the K edge for lead at 88 keV (Fig. 18.12) means that the work of removing an electron from the K shell, where it experiences the field of the nearly unshielded nuclear charge of the lead nucleus, is 88 keV. The screening for lead

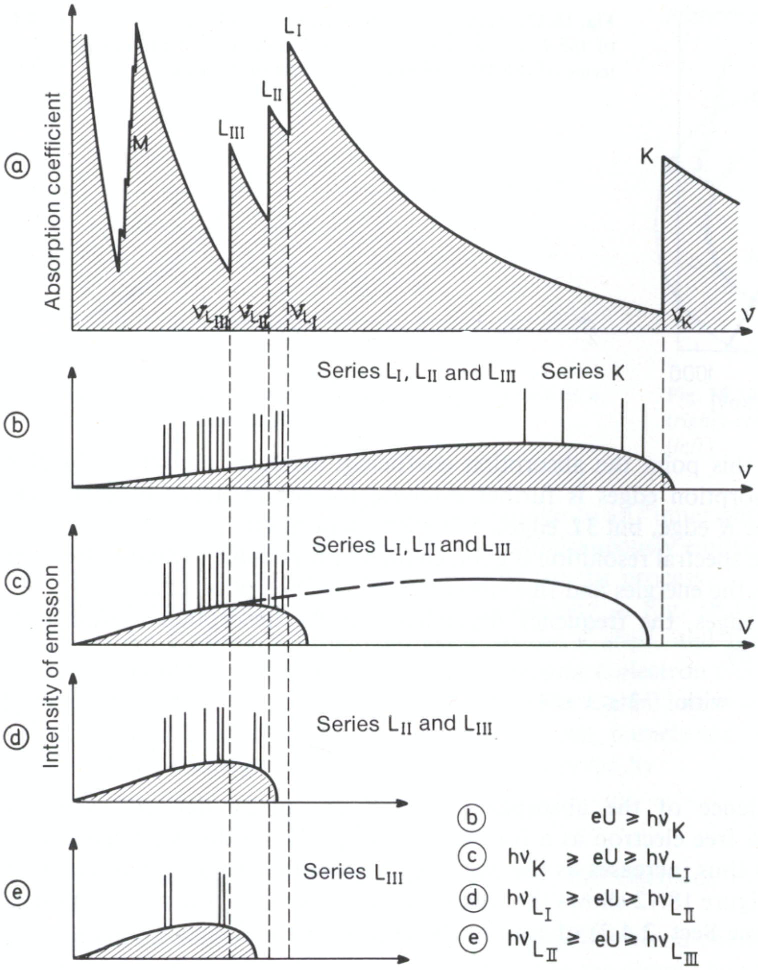

Fig. 18.11 a–e. Comparison of x-ray absorption and emission spectra. **a)** Absorption coefficient, e.g. of platinum for x-rays, as a function of frequency, schematically. The spectrum consists primarily of superimposed absorption edges and series-limit continua. **b–e)** Emission spectrum of platinum at various excitation energies. All the line series are excited in **b**, in **c** the K series is lacking, in **d** the K and L_1 series are absent, and in **e** the K, $L_{\rm I}$ and $L_{\rm II}$ series are missing. The spectral intensity distribution of the continuous (bremsstrahlung) spectrum is modified here, relative to the shape given by (18.1), as a result of frequency-dependent absorption. For platinum, the frequency value of the K edge is ca. $19 \cdot 10^{18}\,\mathrm{s}^{-1}$ and that of the $L_{\rm I}$ edge is ca. $3 \cdot 10^{-18}\,\mathrm{s}^{-1}$

($Z = 82$) can be calculated. For the innermost electron, the work of separation is $Z_{\rm eff}^2 \cdot 13.6$, where $Z_{\rm eff} \equiv Z - s$ is the effective nuclear charge and 13.6 eV is the ionisation energy for the hydrogen atom (Sect. 8.4). From $(82 - s)^2 \cdot 13.6$ eV = 88 keV, $s = 1.61$.

In order for an atom to absorb x-radiation, an electron must be excited from an inner shell into a less strongly bound state. Since the neighbouring shells are already occupied, discrete absorption lines due to transitions from one shell into another are scarcely observable. There is, however, a continuum of free states on the other side of the series limit into which the absorbing electron can be lifted. Therefore, absorption is usually associated with ionisation, and the absorption spectra are the superimposed series-limit continua of the various shells and subshells. This is shown in Fig. 18.11.

Going from lower to higher frequencies, absorption edges, or jumps in the absorption coefficient, are located at those points where the energy of the x-ray quantum is just sufficient to allow an absorptive transition from a new (lower) shell into the limiting continuum.

At lower frequencies, the quantum energy $h\nu$ is only sufficient to release electrons from outer shells. As $h\nu$ increases, an energy is reached which is sufficient to release even

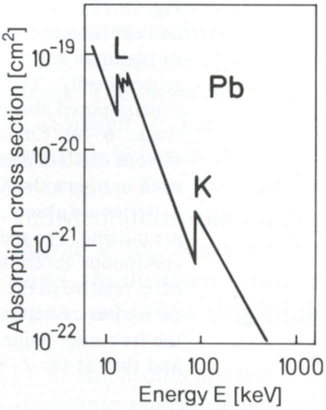

Fig. 18.12. Absorption cross section of lead for x-rays in the region of the *L* and *K* edges. The absorption coefficient is expressed in terms of the absorption cross section of an atom

K electrons, and at this point the absorption coefficient increases abruptly. The fine structure of the absorption edges is further evidence for the existence of shells and subshells: there is one *K* edge, but 3 *L* edges, 5 *M* edges, and so on.

In addition, if the spectral resolution is good enough, it is possible to detect effects of chemical bonding on the energies and fine structures of the absorption edges.

Aside from the edges, the frequency dependence of the absorption coefficient is essentially expressed by

$$\mu_{\text{abs}} \cong Z^x/(h\nu)^3 \quad \text{with} \quad 3 \lesssim x \lesssim 4 \tag{18.5}$$

or $\mu_{\text{abs}} \cong \lambda^3 Z^x$.

The ν^{-3}-dependence of the absorption coefficient can be derived using the Hertzian model of a free electron as a forced oscillator. The hardness or penetrating ability of the x-rays thus increases as the wavelength decreases, or as the accelerating voltage increases. Figure 18.12 shows the frequency dependence of the atomic absorption cross section (see Sect. 2.4.2) of lead in the region of the *K* and *L* edges.

18.7 The Auger Effect

Not all atoms from which electrons have been removed from inner shells by electron bombardment or other forms of energy transfer return to the ground state by emitting x-rays. Instead, the observed quantum yield for x-ray emission is frequently less than 1. It is defined here as

$$\eta = \frac{\text{Number of x-ray emitting atoms}}{\text{Number of } K, L \ldots \text{ ionised atoms}} .$$

Thus it must be possible for the atoms to return to the ground state without emitting radiation. The probability of such non-radiative processes, which compete with x-ray emission, has been found to decrease with increasing nuclear charge. In light atoms, the non-radiative processes far outweigh emittive processes (Fig. 18.13).

The non-radiative return to ground state is accomplished by the *Auger effect*. After an electron has been removed from an inner shell, the excess energy can be released either in the form of an x-ray quantum or through the emission of an electron from a

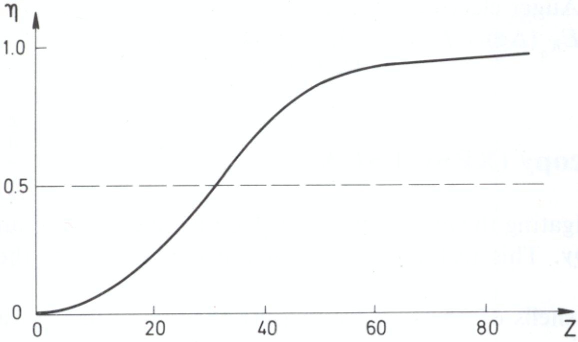

Fig. 18.13. The quantum yield for the emission of x-rays as a function of the Z number (schematically)

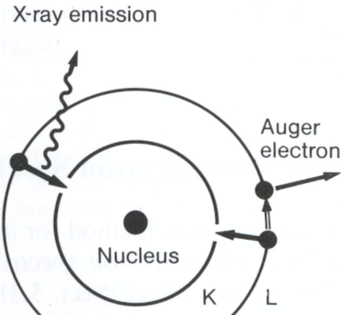

Fig. 18.14. Auger electron emission (*right*) competes with x-ray emission (*left*)

shell farther out. The Auger effect is thus similar to an "inner photoeffect". If one electron falls into a lower shell and another is simultaneously emitted, the Coulomb interaction between the two must be responsible for the process.

The Auger effect is represented schematically in Fig. 18.14. First the K shell is ionised. An L electron falls from the L to the K shell, and fills the hole there. The energy released by this is used to remove a second L electron from the L shell, and this one escapes from the atom. The result is that the L shell loses two electrons. These are then replaced by electrons from shells farther out, namely the M shell and so on.

The kinetic energy of the Auger electron is given by

$$E_{\text{kin}} = h\nu_{K_\alpha} - E_L = E_K - E_L - E_L = E_K - 2E_L\,, \tag{18.6}$$

where E_L and E_K are the binding energy of the electrons in the L and K shells, respectively.

Auger electrons can also be observed directly in a cloud chamber. Their energy can be determined from the length of their tracks in the cloud chamber, or by means of a braking field method, and thus can be used to verify the explanation of the Auger effect.

Finally, a numerical example: Silver is bombarded with K_α radiation from a tungsten anticathode (energy = 59.1 keV). Electrons with the following energies are observed:

1) 55.8 keV Interpretation: Photoelectrons from the Ag L shell
Because: the ionisation energy of the Ag L shell is $E_{\text{ion}L} = 3.34$ keV
Therefore: $59.1 - 3.34 = 55.76$ keV.

2) 33.8 keV Interpretation: Photoelectrons from the Ag K shell
Because: $E_{\text{ion}K} = 25.4$ keV
Therefore: $59.1 - 25.4 = 33.7$ keV.

3) 21.3 keV Interpretation: Auger electrons
Because: $E_{K_\beta}(\text{Ag}) - E_{\text{ion}L} = 24.9 - 3.34$
$= 21.56$ keV.

4) 18.6 keV Interpretation: Auger electrons

$$\text{Because: } E_{K_\alpha}(\mathrm{Ag}) - E_{\mathrm{ion}\,L} = 22.1 - 3.34 = 18.76\ \mathrm{keV}.$$

18.8 Photoelectron Spectroscopy (XPS), ESCA

A relatively new method for investigating the energy states of the inner electrons of an atom is *photoelectron spectroscopy*. This technique is a modern application of the photoelectric effect (Sect. 5.3).

Electrons are ejected from the shells of an atom by exciting them with light of a known quantum energy. The kinetic energies of the photoelectrons correspond to the difference between the quantum energy of the photons and the binding energies of the electrons in the atom, following the energy-balance equation of the photoelectric effect, $E_{\mathrm{kin}} = h\nu - E_{\mathrm{bind}}$. The principle is illustrated in Fig. 18.15. Figure 18.16 shows as an example the binding energies in some light atoms. An example of a measurement for the Hg atom is given in Fig. 18.17. With this method, the binding energies of inner-shell electrons can be determined directly, in contrast to x-ray absorption spectroscopy, which gives only the energy of the absorption edge.

The measurement of the kinetic energy of the photoelectrons is performed with high-resolution analysers, which allow a precise determination of the velocities of the electrons using the principle of the determination of e/m (deflection in electric and magnetic fields) described in Sect. 6.4. (Simultaneous measurement over a wide range of electron kinetic energies is also possible using time-of-flight analysers, with somewhat poorer energy resolution.) The best energy resolutions currently available allow determination of the electron energies to about 20 meV.

The light source provides either UV light of short wavelengths, e.g. the resonance lines from the Ne and the He spectra in the region between 15 and 50 eV, or else, for the

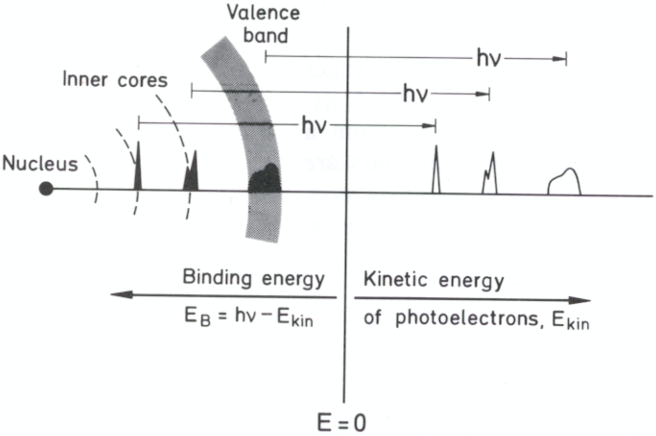

Fig. 18.15. Illustration of photoelectron spectroscopy. The kinetic energy of the photoelectrons is the difference between the quantum energy $h\nu$ of the excitation photons and the binding energy of the electrons in an atom or a solid. The dashed lines represent the orbitals of the electrons. One should note, however, that here the binding energies, and not the distance from the nucleus, are indicated

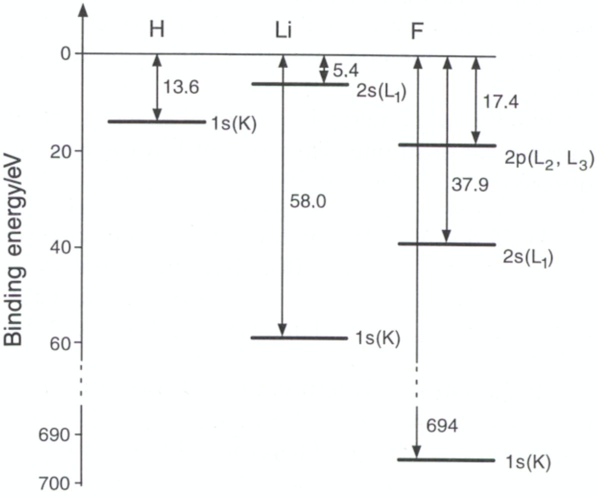

Fig. 18.16. Binding energy of the electrons in the H, Li, and F atoms; the atomic K, L_1, L_2, and L_3 shells are indicated. The zero point for the binding energy is the ionisation limit

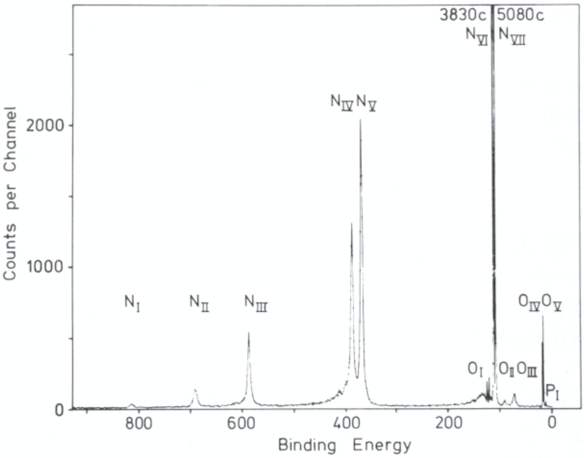

Fig. 18.17. The photoelectron spectrum of Hg vapour, after K. Siegbahn (overview of the spectrum). All the levels which can be excited with the K_α radiation from Al are to be seen. These are the N and O shells, as well as P_I. Compare also the electron configuration of the Hg atom from Table 19.3b

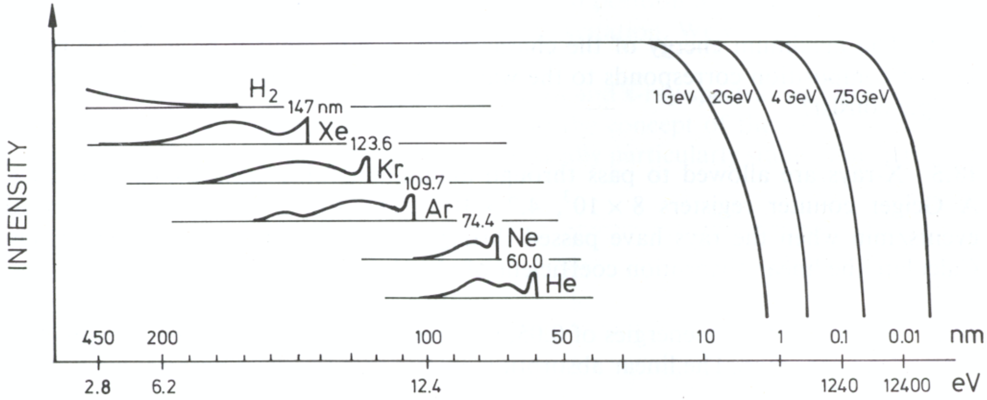

Fig. 18.18. The spectral distributions of different excitation light sources for photoelectron spectroscopy and of synchrotron radiation from different primary electron energies. The ordinate scales are in arbitrary units and are each different. After Bethge and Gruber

investigation of states with higher binding energies, the characteristic x-ray lines, e.g. the K_α lines from Cu (8048 eV), from Al (1487 eV), or from Mg (1254 eV). Synchrotron radiation, which has a continuously variable photon energy in the whole UV and x-ray region (cf. Sect. 5.1), is a particularly suitable light source. An overview is given in Fig. 18.18.

The binding energies of the electrons are characteristic of the particular atoms being investigated, so that the method can also be used for *chemical analysis* of a sample. Furthermore, the chemical bonding between atoms in molecules or in solids leads to a redistribution of the valence electrons. This, in turn, changes the entire bonding potential in the atoms, whereby even the inner electrons are affected. The resulting small shifts in the inner-shell binding energies due to changes in the state of the outer (valence) electrons are termed *chemical shifts* and can be measured, e.g. between atoms in different ionisation states. The corresponding analytical method, called ESCA (*E*lectron *S*pectroscopy for *C*hemical *A*nalysis), was developed in particular by *K. Siegbahn* and coworkers. It has become an important experimental technique in chemistry and in molecular and solid state physics.

Problems

18.1 What is the shortest possible wavelength for bremsstrahlung observed when an electron which has been accelerated through a potential difference of 40 kV is stopped by the anticathode of an x-ray tube? In what region of the electromagnetic spectrum does this wavelength lie?

18.2 The K_α line of cobalt is at 1.785 Å. What is the energy difference between the $1s$ and $2p$ orbitals in cobalt? Compare this result with the energy difference between the $1s$ and $2p$ orbitals in hydrogen (that is, the first Lyman line). Why is the difference much greater for cobalt than for hydrogen?

18.3 The most intense line in the x-ray spectrum arises from the transition in which an electron goes from the shell with $n = 2$ to the shell with $n = 1$. The transition is described by Moseleys rule (cf. Sect. 18.4). What is the wavelength of this line for copper?

18.4 The maximum energy of the characteristic x-rays emitted by a sample of unknown composition corresponds to the wavelength 2.16 Å. Of what element does the sample consist?

18.5 X-rays are allowed to pass through aluminium foils, each 4×10^{-3} m thick. A Geiger counter registers 8×10^3, 4.7×10^3, 2.8×10^3, 1.65×10^3 and 9.7×10^2 events/min when the rays have passed through 0, 1, 2, 3 and 4 foils, respectively. Calculate the linear absorption coefficient of aluminium.

18.6 Gamma rays with energies of 0.05, 0.3 and 1 MeV, but the same intensities, fall onto a lead absorber. The linear absorption coefficients for these energies are 8×10^3, 5×10^2 and 78 m^{-1}.

a) Calculate the thickness of lead required to reduce the intensity of each beam of gamma rays to one tenth of its original value.
b) What is the relation of the total intensity (at each photon energy) at a depth of 5 mm to the total incident intensity?

18.7 How many times the half-absorption thickness of a material is required to reduce the intensity of an x-ray beam to (a) 1/16, (b) 1/20, or (c) 1/200 of the incident intensity?

18.8 a) The K absorption edge of tungsten is at 0.178 Å, and the wavelengths of the lines of the K series are (ignoring the fine structure) $K_\alpha = 0.210$ Å, $K_\beta = 0.184$ Å, and $K_\gamma = 0.179$ Å. Sketch the energy levels of W and give the energies of the K, L, M and N shells.

b) What is the minimum energy required to excite the L series in tungsten? What is the wavelength of the L line?

18.9 The L_I absorption edge in tungsten is at 1.02 Å. Assume that a K_α photon is "absorbed" by one of the $2s$ electrons by an Auger process. Determine the velocity of the photoelectron released.

19. Structure of the Periodic System. Ground States of the Elements

19.1 Periodic System and Shell Structure

It is one of the goals of atomic physics to understand the ordering and the properties of the chemical elements in the periodic system. The empirically determined physical and chemical properties of the atoms and their dependence on the atomic number Z ought to be explainable starting from the electronic structures of the atoms. After having, in the previous chapters, discussed one-electron spectra, many-electron spectra, and the spectra of the inner shells in detail, we are now in a position to understand, at least in principle, the spectra of any atom in any state of excitation. We will outline and extend this understanding in the present chapter.

In particular, in the discussions of alkali atoms and x-ray spectra, we have met with some important experimental facts which led to the concept of the shell structure of atoms. It is known that the noble gases are chemically particularly stable. Furthermore,

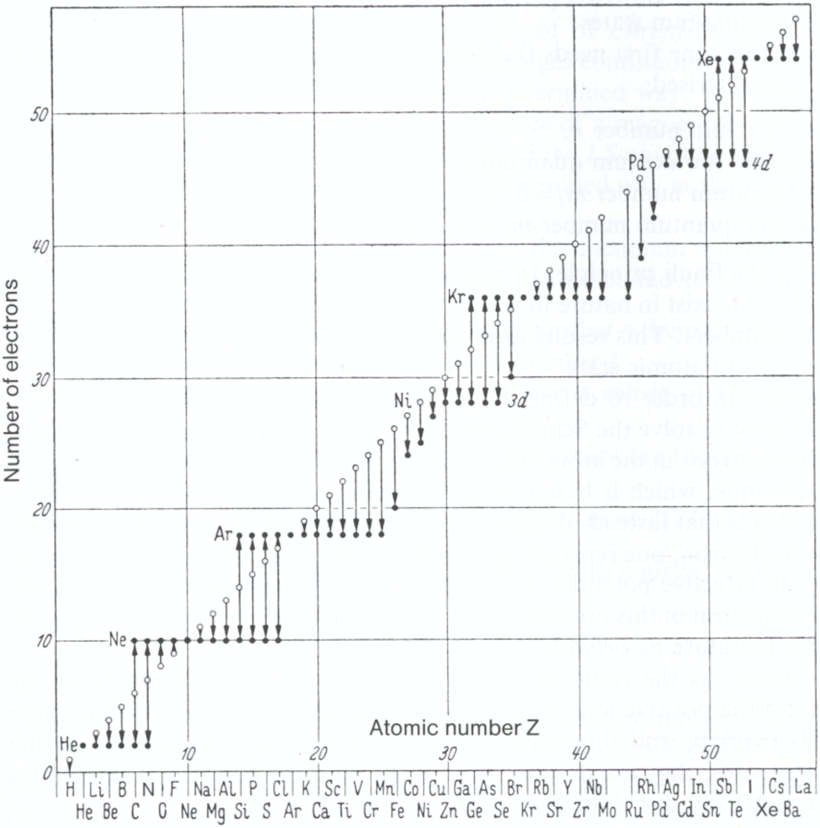

Fig. 19.1. Electronic shells of the ions of atoms, following *Kossel*, 1916. The number of electrons is plotted against the nuclear charge number for atoms and for the ions which are preferentially formed from those atoms in chemical bonding. The electronic shells of the atoms are depleted or filled up to the electron numbers indicated by arrows in the diagram when ions are formed. With the exceptions of nickel and palladium, the preferred electron numbers are those of the noble gases. [From K. H. Hellwege: *Einführung in die Physik der Atome*, Heidelberger Taschenbücher, Vol. 2, 4th ed. (Springer, Berlin, Heidelberg, New York 1974) Fig. 61]

if the electrochemical valency of an ion is compared to the distance of the corresponding neutral element from the nearest noble gas in the periodic table, it is found that the atoms have been ionised to such an extent that the ions have assumed the electron number of a neutral noble gas. The observed ionisation levels of the atoms are shown in a way that makes this clear in Fig. 19.1. Thus when an ion is formed, those electrons which are in excess of the electron number of a noble gas are most easily lost, or the electrons which are lacking from the electron number of the next heavier noble gas are most easily acquired. Consider, for example, the elements around the noble gas neon ($Z = 10$). The next element in the periodic table is sodium ($Z = 11$), which preferentially forms singly charged positive ions. The next element, magnesium ($Z = 12$), forms doubly charged positive ions. The next lighter element than neon, fluorine ($Z = 9$), forms singly charged negative ions (by acquisition of an electron) and so on.

It can be seen from Fig. 19.1 that nickel and palladium also have preferred electron numbers, because the atoms of neighbouring elements tend to assume these numbers when they become ionised. The stable electron configurations are thus not limited to the noble gases. This is made clear in the discussion of Table 19.3.

We know from the spectroscopic studies of atoms discussed in earlier chapters that the unusually stable electron configurations are characterised by complete mutual compensation of all angular momenta and magnetic moments. Furthermore, the shell and subshell structure of the electron distribution of atoms appears especially clearly in x-ray spectra as a system of absorption edges.

We now turn to the question of which electronic configurations are possible in atoms, which are particularly stable, and how the electrons of an atom are distributed among the possible quantum states.

To understand this, one first needs the quantum numbers with which each atomic electron can be characterised:

the principal quantum number n,
the orbital angular momentum quantum number $l = 0, 1 \ldots n-1$,
the magnetic quantum number $m_l = 0, \pm 1 \ldots \pm l$,
the magnetic spin quantum number $m_s = \pm 1/2$.

One also needs the Pauli principle. In non-mathematical terms, this says that only those atomic states can exist in nature in which any two electrons differ, in at least one of their quantum numbers. This results in limitations in the possible combinations of quantum numbers in an atomic state.

Strictly speaking, in order to define the quantum numbers of an electron in the atom, one would have to solve the Schrödinger equation for a many-particle problem, namely for all the electrons in the atom. The problem is solved approximately using the Hartree-Fock technique, which is based on the model of independent particles (Sect. 19.4). The basic idea is that instead of trying to calculate the interactions of $N-1$ electrons with the Nth electron, one replaces the Coulomb attraction of the nucleus for the Nth electron by an effective potential. One then calculates the eigenstates and eigenvalues of the Nth electron in this potential field. These one-particle functions are often referred to in the literature as *orbitals*.

Figure 19.2 shows, as the result of such calculations, the shell structure of the hydrogen atom and the positive ions of lithium, sodium and potassium. As the figure shows, the shells overlap, and thus have no unique geometric significance. As the nuclear charge increases, they are drawn closer to the nucleus. Another example of a calculated electron density distribution was discussed in Fig. 11.8.

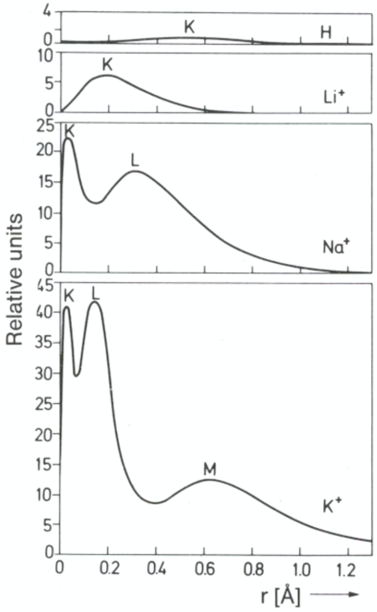

Fig. 19.2. Radial density distribution of electrons in the hydrogen atom, and the singly charged positive ions of lithium, sodium and potassium. It is especially noticeable how the *K* shell electrons move closer to the nucleus as the nuclear charge increases

In the absence of an external magnetic field, the magnetic quantum numbers would seem to lose their function, because of degeneracy. In order to apply the Pauli principle to atomic terms in such cases, we make use of of *Ehrenfest*'s adiabatic invariance principle, which states that if a parameter changes continuously, the states of an atom also change in a continuous and uniquely determined way. In the present case, this means that the states of the atom in the absence of a magnetic field must derive from those in the presence of a strong field – where the *LS*-coupling and the *m*-degeneracy are lifted – in a continuous and uniquely determined way as the field is slowly turned off.

With the Pauli principle it is easy to count the maximum number of electrons with a given principal quantum number n which can be bound to an atom:

- For a given value of the principal quantum number n there are n different values for the orbital angular momentum quantum number l.
- For every value of l there are $2l+1$ different values of the magnetic quantum number m_l.
- For each pair of quantum numbers l and m_l there are two different values of the spin quantum number m_s.
- Thus for each pair of numbers n, l there are at most $2(2l+1)$ electrons.

The maximum number of electrons in a shell with a given value of n is then

$$\sum_{l=0}^{n-1} 2(2l+1) = 2n^2 . \qquad (19.1)$$

Table 19.1 gives the possible combinations of quantum numbers for $n = 1$, 2 and 3.

If a *shell* is defined as the group of all electrons with the same principal quantum number n, then the atoms with closed shells are helium ($n = 1$), neon ($n = 2$), nickel ($n = 3$, $Z = 28$) and neodymium ($n = 4$, $Z = 60$). Nickel and neodymium are neither

Table 19.1. Possible quantum numbers and numbers of electrons in the shells with $n = 1, 2, 3$

n	l	m_l	m_s	Number of electrons		Configuration	Shell
1	0	0	$\pm 1/2$	2		$1s^2$	K shell
2	0	0	$\pm 1/2$	$1 \cdot 2$		$2s^2p^6$	L shell
	1	1	$\pm 1/2$		$= 8$		
		0	$\pm 1/2$				
		-1	$\pm 1/2$	$3 \cdot 2$			
3	0	0	$\pm 1/2$	$1 \cdot 2$			
	1	1	$\pm 1/2$				
		0	$\pm 1/2$				
		-1	$\pm 1/2$	$3 \cdot 2$			
	2	2	$\pm 1/2$		$= 18$	$3s^2p^6d^{10}$	M shell
		1	$\pm 1/2$				
		0	$\pm 1/2$				
		-1	$\pm 1/2$				
		-2	$\pm 1/2$	$5 \cdot 2$			

noble gases nor chemically very inactive. The simple equation of a closed shell with a noble gas configuration breaks down for higher electron numbers. In the He atom, the *K* shell is fully occupied; in Ne, the *K* and *L* shells; and in Ar, also the *s*- and *p*-suborbitals of the *M* shell.

Instead, it is observed that the closure of a *partial shell*, that is occupation of all states with the same value of l for a given value of n, leads to especially stable electron configurations. This is understandable in light of the fact that even for fully occupied partial shells, the angular momentum and magnetic moments add up to zero, so that the atom is outwardly spherically symmetric. In fact, this is the case with the third noble gas, argon, which has the electronic configuration $1s^2\,2s^2\,2p^6\,3s^2\,3p^6$. In other words, all of the *s* and *p* electrons are present in the third shell, but there are no *d* electrons. The cases of the noble gases krypton and xenon are similar, as is shown in Table 19.2.

Table 19.2. Electronic configuration for the highest occupied shells or partial shells of the noble gases. Only helium and neon have completely filled highest shells. The particular stability of the other noble gases is due to completion of partial shells

Highest occupied state	Z	Element	1st ionisation potential [eV]
$(1s)^2$	2	He	24.58
$(2s)^2(2p)^6$	10	Ne	21.56
$(3s)^2(3p)^6$	18	Ar	15.76
$(4s)^2(3d)^{10}(4p)^6$	36	Kr	14.00
$(5s)^2(4d)^{10}(5p)^6$	54	Xe	12.13
$(6s)^2(4f)^{14}(5d)^{10}(6p)^6$	86	Rn	10.75

Having seen that each partial or complete shell can only accommodate a certain maximum number of electrons, we can turn to the configurations of all the atoms of the periodic system. Table 19.3 a and b shows all the elements with their electronic configurations. Closed complete and partial shells are shaded in. The table also shows the first ionisation energy for each element.

With increasing atomic number Z, the added electrons successively occupy the unfilled shells and subshells. The order of this filling depends on the binding energies; in particular, for heavy atoms it does not correspond simply to the numerical order. The first deviation is found in the K atom: there, it is energetically more favorable for the last electron to occupy the $4s$ subshell rather than the $3d$. Compare also Sect. 11.3.

The interaction energies of the electrons with the nucleus and with each other, which play a key rôle in determining the energetic positions of the subshells and thus the structure of the Periodic Table, are dominated for lighter elements by purely electrostatic interactions, particularly screening of the nuclear charge by the other electrons. With increasing atomic number Z, the magnetic interactions, specifically the spin-orbit interaction, become comparably large and, for the heaviest elements, finally determine the ordering of the electronic states.

Figure 19.3 again summarises the energetic ordering of the subshells for the successive addition of electrons, corresponding to the shell structure. It is characterised by the fact that at certain energies, large gaps between the energy levels are found. These mark the especially stable configurations, for example those of the noble gases.

The shell structure that we have described here, which is important for understanding the Periodic System, is – as we again emphasize – that of the *last electron* added to the atom. When the initially outermost electrons move inwards, as the atomic number increases and further electrons are added to the outer shells, they become more and more subject to the effective potential of the other electrons and the ordering of their energy levels changes. This is illustrated in Fig. 19.3. The energetic order of the subshells then becomes a function of the principal quantum number n only. This shell structure, determined only by n, is the one we have already met with in treating the x-ray spectra of atoms. It can also be investigated using photoelectron spectroscopy.

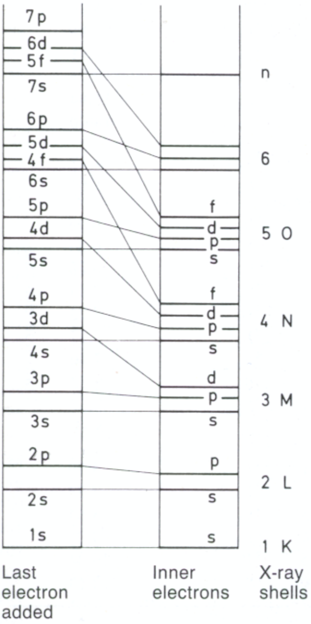

Fig. 19.3. The shell structure of the atomic energy levels and their ordering, for the last added electron and for the inner electrons. Especially stable configurations are those in which a large energy gap to the next level occurs

Table 19.3 a. Periodic Table with electron configurations, ground state terms, and ionisation energies. The filled shells and subshells are shaded

Atomic number Z	Element		Shells											*LS* configuration of the ground state	First ionisation potential [eV]	
			K	*L*		*M*			*N*			*O*				
			$n=1$	$n=2$		$n=3$			$n=4$			$n=5$				
			s	*s*	*p*	*s*	*p*	*d*	*s*	*p*	*d*	*s*	*p*			
1	Hydrogen	H	1											$^2S_{1/2}$	13.60	
2	Helium	He	2											$^1S_0$	24.58	
3	Lithium	Li	2	1										$^2S_{1/2}$	5.39	
4	Beryllium	Be	2	2										$^1S_0$	9.32	
5	Boron	B	2	2	1									$^2P_{1/2}$	8.30	
6	Carbon	C	2	2	2									$^3P_0$	11.26	
7	Nitrogen	N	2	2	3									$^4S_{3/2}$	14.54	
8	Oxygen	O	2	2	4									$^3P_2$	13.61	
9	Fluorine	F	2	2	5									$^2P_{3/2}$	17.42	
10	Neon	Ne	2	2	6									$^1S_0$	21.56	
11	Sodium	Na	2	2	6	1								$^2S_{1/2}$	5.14	
12	Magnesium	Mg	2	2	6	2								$^1S_0$	7.64	
13	Aluminium	Al	2	2	6	2	1							$^2P_{1/2}$	5.98	
14	Silicon	Si	2	2	6	2	2							$^3P_0$	8.15	
15	Phosphorous	P	2	2	6	2	3							$^4S_{3/2}$	10.55	
16	Sulphur	S	2	2	6	2	4							$^3P_2$	10.36	
17	Chlorine	Cl	2	2	6	2	5							$^2P_{3/2}$	13.01	
18	Argon	Ar	2	2	6	2	6							$^1S_0$	15.76	
19	Potassium	K	2	2	6	2	6		1					$^2S_{1/2}$	4.34	
20	Calcium	Ca	2	2	6	2	6		2					$^1S_0$	6.11	
21	Scandium	Sc	2	2	6	2	6	1	2					$^2D_{3/2}$	6.56	Transition elements
22	Titanium	Ti	2	2	6	2	6	2	2					$^3F_2$	6.83	
23	Vanadium	V	2	2	6	2	6	3	2					$^4F_{3/2}$	6.74	
24	Chromium	Cr	2	2	6	2	6	5	1					$^7S_3$	6.76	
25	Manganese	Mn	2	2	6	2	6	5	2					$^6S_{5/2}$	7.43	
26	Iron	Fe	2	2	6	2	6	6	2					$^5D_4$	7.90	
27	Cobalt	Co	2	2	6	2	6	7	2					$^4F_{9/2}$	7.86	
28	Nickel	Ni	2	2	6	2	6	8	2					$^3F_4$	7.63	
29	Copper	Cu	2	2	6	2	6	10	1					$^2S_{1/2}$	7.72	
30	Zinc	Zn	2	2	6	2	6	10	2					$^1S_0$	9.39	
31	Gallium	Ga	2	2	6	2	6	10	2	1				$^2P_{1/2}$	6.00	
32	Germanium	Ge	2	2	6	2	6	10	2	2				$^3P_0$	7.88	
33	Arsenic	As	2	2	6	2	6	10	2	3				$^4S_{3/2}$	9.81	
34	Selenium	Se	2	2	6	2	6	10	2	4				$^3P_2$	9.75	
35	Bromine	Br	2	2	6	2	6	10	2	5				$^2P_{3/2}$	11.84	
36	Krypton	Kr	2	2	6	2	6	10	2	6				$^1S_0$	14.00	
37	Rubidium	Rb	2	2	6	2	6	10	2	6		1		$^2S_{1/2}$	4.18	
38	Strontium	Sr	2	2	6	2	6	10	2	6		2		$^1S_0$	5.69	
39	Yttrium	Y	2	2	6	2	6	10	2	6	1	2		$^2D_{3/2}$	6.38	Transition elements
40	Zirconium	Zr	2	2	6	2	6	10	2	6	2	2		$^3F_2$	6.84	
41	Niobium	Nb	2	2	6	2	6	10	2	6	4	1		$^6D_{1/2}$	6.88	
42	Molybdenum	Mo	2	2	6	2	6	10	2	6	5	1		$^7S_3$	7.13	
43	Technetium	Tc	2	2	6	2	6	10	2	6	6	1		$^6D_{9/2}$	7.23	
44	Ruthenium	Ru	2	2	6	2	6	10	2	6	7	1		$^5F_5$	7.37	
45	Rhodium	Rh	2	2	6	2	6	10	2	6	8	1		$^4F_{9/2}$	7.46	
46	Palladium	Pd	2	2	6	2	6	10	2	6	10			$^1S_0$	8.33	
47	Silver	Ag	2	2	6	2	6	10	2	6	10	1		$^2S_{1/2}$	7.57	
48	Cadmium	Cd	2	2	6	2	6	10	2	6	10	2		$^1S_0$	8.99	
49	Indium	In	2	2	6	2	6	10	2	6	10	2	1	$^2P_{1/2}$	5.79	
50	Tin	Sn	2	2	6	2	6	10	2	6	10	2	2	$^3P_0$	7.33	
51	Antimony	Sb	2	2	6	2	6	10	2	6	10	2	3	$^4S_{3/2}$	8.64	
52	Tellurium	Te	2	2	6	2	6	10	2	6	10	2	4	$^3P_2$	9.01	
53	Iodine	J	2	2	6	2	6	10	2	6	10	2	5	$^2P_{3/2}$	10.44	
54	Xenon	Xe	2	2	6	2	6	10	2	6	10	2	6	$^1S_0$	12.13	

Table 19.3b. Periodic Table with electron configurations, ground state terms, and ionisation energies. The filled shells and subshells are shaded. (The subshells $5g$ and $6f$, $6g$, $6h$ are not shown, since there are no atoms which have electrons in these shells in their ground states). The transuranium elements with atomic numbers from 106 to 118, which have recently been artificially produced, are not shown here

Atomic number Z	Element		Shells N $n=4$ s	p	d	f	O $n=5$ s	p	d	f	P $n=6$ s	p	d	Q $n=7$ s	LS configuration of the ground state	First ionisation potential [eV]	
55	Cesium	Cs	2	6	10		2	6			1				$^2S_{1/2}$	3.89	
56	Barium	Ba	2	6	10		2	6			2				$^1S_0$	5.21	
57	Lanthanum	La	2	6	10		2	6	1		2				$^2D_{3/2}$	5.61	Rare earths
58	Cerium	Ce	2	6	10	2	2	6			2				$^3H_4$	5.6	
59	Praseodymium	Pr	2	6	10	3	2	6			2				$^4I_{9/2}$	5.46	
60	Neodymium	Nd	2	6	10	4	2	6			2				$^5I_4$	5.51	
61	Promethium	Pm	2	6	10	5	2	6			2				$^6H_{5/2}$		
62	Samarium	Sm	2	6	10	6	2	6			2				$^7F_0$	5.6	
63	Europium	Eu	2	6	10	7	2	6			2				$^8S_{7/2}$	5.67	
64	Gadolinium	Gd	2	6	10	7	2	6	1		2				$^9D_2$	6.16	
65	Terbium	Tb	2	6	10	9	2	6			2				—	5.98	
66	Dysprosium	Dy	2	6	10	10	2	6			2				$^5I_8$	6.8	
67	Holmium	Ho	2	6	10	11	2	6			2				$^4I_{15/2}$		
68	Erbium	Er	2	6	10	12	2	6			2				$^3H_6$	6.08	
69	Thulium	Tm	2	6	10	13	2	6			2				$^2F_{7/2}$	5.81	
70	Ytterbium	Yb	2	6	10	14	2	6			2				$^1S_0$	6.22	
71	Lutetium	Lu	2	6	10	14	2	6	1		2				$^2D_{3/2}$	6.15	Transition elements
72	Hafnium	Hf	2	6	10	14	2	6	2		2				$^3F_2$	5.5	
73	Tantalum	Ta	2	6	10	14	2	6	3		2				$^4F_{3/2}$	7.7	
74	Tungsten	W	2	6	10	14	2	6	4		2				$^5D_0$	7.98	
75	Rhenium	Re	2	6	10	14	2	6	5		2				$^6S_{5/2}$	7.87	
76	Osmium	Os	2	6	10	14	2	6	6		2				$^5D_4$	8.7	
77	Iridium	Ir	2	6	10	14	2	6	9						$^2D_{5/2}$	9.2	
78	Platinum	Pt	2	6	10	14	2	6	9		1				$^3D_3$	9.0	
79	Gold	Au	2	6	10	14	2	6	10		1				$^2S_{1/2}$	9.22	
80	Mercury	Hg	2	6	10	14	2	6	10		2				$^1S_0$	10.43	
81	Thallium	Tl	2	6	10	14	2	6	10		2	1			$^2P_{1/2}$	6.11	
82	Lead	Pb	2	6	10	14	2	6	10		2	2			$^3P_0$	7.42	
83	Bismuth	Bi	2	6	10	14	2	6	10		2	3			$^4S_{3/2}$	7.29	
84	Polonium	Po	2	6	10	14	2	6	10		2	4			$^3P_2$	8.43	
85	Astatine	At	2	6	10	14	2	6	10		2	5				9.5	
86	Radon	Rn	2	6	10	14	2	6	10		2	6			$^1S_0$	10.75	
87	Francium	Fr	2	6	10	14	2	6	10		2	6		1		4	
88	Radium	Ra	2	6	10	14	2	6	10		2	6		2		5.28	
89	Actinium	Ac	2	6	10	14	2	6	10		2	6	1	2			Actinides
90	Thorium	Th	2	6	10	14	2	6	10		2	6	2	2			
91	Protactinium	Pa	2	6	10	14	2	6	10	2	2	6	1	2			
92	Uranium	U	2	6	10	14	2	6	10	3	2	6	1	2			
93	Neptunium	Np	2	6	10	14	2	6	10	4	2	6	1	2			
94	Plutonium	Pu	2	6	10	14	2	6	10	6	2	6		2			
95	Americium	Am	2	6	10	14	2	6	10	7	2	6		2			
96	Curium	Cm	2	6	10	14	2	6	10	7	2	6	1	2			
97	Berkelium	Bk	2	6	10	14	2	6	10	8	2	6	1	2			
98	Californium	Cf	2	6	10	14	2	6	10	10	2	6		2			
99	Einsteinium	Es	2	6	10	14	2	6	10	11	2	6		2			
100	Fermium	Fm	2	6	10	14	2	6	10	12	2	6		2			
101	Mendelevium	Md	2	6	10	14	2	6	10	13	2	6		2			
102	Nobelium	No	2	6	10	14	2	6	10	14	2	6		2			
103	Lawrencium	Lr	2	6	10	14	2	6	10	14	2	6	1	2			
104	Rutherfordium	Rf	2	6	10	14	2	6	10	14	2	6	2	2			
105	Dubnium	Db	2	6	10	14	2	6	10	14	2	6	3	2			

As discussed in Sect. 18.8, this is a technique for studying quantitatively the binding energies of the inner (and outer) electrons of atoms.

The occupation of the shells and subshells is responsible for the physical and chemical properties of the atoms. The alkali atoms Li, Na, K, Rb, Cs, and Fr have a single electron in a newly-begun shell, i.e. in the *L* shell, the *M* shell, the 4*s* subshell of the *N* shell, etc. They are therefore easily ionised – they have low ionisation potentials – and are chemically monovalent. The halogen atoms F, Cl, Br, and I are also monovalent: here, just one electron is lacking to fill the outermost *p* subshell in the *L*, *M*, *N*, and *O* shells, respectively. As a result, these elements have a large electron affinity; this means that the "electronic hole" can easily be filled as a result of a chemical reaction.

The changed energetic ordering of the subshells is especially noticeable in the case of the transition elements and the rare earths. The elements of the first transition series from Sc to Ni owe their characteristic properties, such as their colours and paramagnetism, to their partially-filled 3*d* shells. Their chemical valence is determined by the outer (valence) electrons. Since these are close neighbours to the 3*d* electrons, the latter can readily switch between shells, giving the transition elements a variety of different possible valencies.

A similar picture is found for the second transition series or 4*d* transition elements, $_{39}$Y through $_{46}$Pd, as well as for the 4*f* transition elements, the lanthanoids or rare earths $_{57}$La through $_{70}$Yb, where the 4*f* subshell is being filled while the 6*s* subshell is already full; for the 5*d* elements $_{71}$Lu through $_{78}$Pt; and for the 5*f* elements (actinoids) $_{91}$Pa through $_{103}$Lr.

The rare earths are the most impressive example of the special properties of atoms in which energetically higher but spatially more contracted shells are being filled. Chemically, they are all very similar, since their valence configurations in the 6*s* (and 5*d*) subshells are identical or quite similar. Their colours and paramagnetism result from their inner 4*f* electrons. The screening of the 4*f* shell by the outer 6*s* electrons is also the reason that the optical spectra of rare earths exhibit sharp lines, even when they are in the solid state. Rare earth atoms or ions in solids are therefore especially well suited as laser media (see Chap. 21). Neodymium has been mainly used for this purpose up to now.

Palladium, with $Z = 46$, is also quite interesting: it has a fully closed subshell configuration. The fact that it is nevertheless not a noble gas becomes understandable when one considers the previous element, rhodium. The 5*s* electron which is still present in Rh has switched to the 4*d* shell in Pd; it requires only a small amount of energy to raise it again to the 5*s* shell. For this reason, Pd is not chemically inactive and not a noble gas, although it is considered to be a noble metal.

19.2 From the Electron Configuration to the Atomic Term Scheme. Atomic Ground States

We are now familiar with the electronic configurations of the atoms, as far as the quantum numbers n and l are concerned. It remains to discuss the energetic order of the states with different values of m_l and m_s and the combination of the angular momenta of individual electrons to form the total angular momentum of the atom.

Figure 19.4 shows the ground states and the electronic configurations of the first 11 elements. For the beryllium and carbon atoms the lowest excited state is also given.

Hydrogen and helium, with the ground states $^2S_{1/2}$ and $^1S_0$ have already been discussed at length. In lithium, the second shell is started, with a $2s$ electron. Beryllium, with a closed $2s$ subshell, has a $^1S_0$ ground state. It can easily be excited to the $2p$ configuration, which is energetically very close to the ground state. The occupation of the $2p$ subshell begins with boron; from its spectrum it is clear that this element has a $^2P_{1/2}$ ground state, i.e. that its orbital and spin angular momenta point in opposite directions. The spectrum of carbon indicates that the spins of the two $2p$ electrons are parallel, so the ground state is $^3P_0$. The excited state C^* shown in Fig. 19.4, in which there are one $2s$ and three $2p$ electrons, is responsible for the valence of 4 which carbon displays in organic chemistry. The four electrons in the second shell are coupled in this state so that they are energetically equivalent. This leads to what is called sp^3 hybridisation (cf. Sect. 23.7) which effectively determines the character of the chemical bonding.

It turns out that in nitrogen, the three p electrons have parallel spins, so that they form a $^4S_{3/2}$ ground state. Spin saturation of the p electrons then begins with oxygen. Fluorine lacks only one electron in the p subshell. With neon, the noble gas ground state $^1S_0$ is reached again. The occupation of the M shell with $n = 3$ begins with the alkali atom sodium.

There are several rules for the energetic ordering of the electrons within the subshells, which hold in addition to the Pauli principle. In LS coupling, i.e. in all light atoms, the angular momenta in the ground state are governed by *Hund's Rules.* They are:

1) Full shells and subshells contribute nothing to the total angular momenta $\boldsymbol{L}$ and $\boldsymbol{S}$. We have already shown this earlier.

2) The electrons having the same value of l which are divided among the corresponding m_l subshells – called equivalent electrons – are placed into the ground state

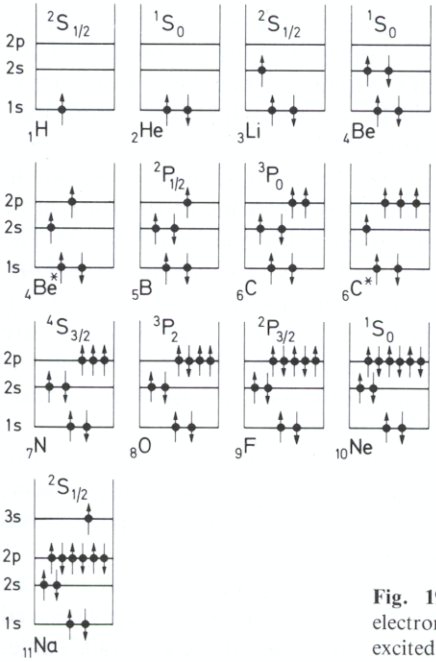

Fig. 19.4. Electronic configurations and arrangement of the electron spins in the ground states of the atoms H to Na. The lowest excited state is also given for beryllium and carbon

in such a way that the resulting total spin S is maximised. States with the highest multiplicities thus lie energetically lowest, e.g. triplet states are lower than singlet states. This is a consequence of the Pauli principle, which requires that the total wavefunction be antisymmetric (see Sects. 19.4, where this "antisymmetry" will be discussed in more detail). The higher the multiplicity, the more parallel spins there are, which are thus completely symmetrical in their symmetry properties. Therefore their spatial functions must be antisymmetric. As a result, their binding energy is maximised, because the mutual Coulomb repulsion of the electrons is lowest for antisymmetric spatial functions.

Let us consider the nitrogen ground state as an example. Nitrogen has three electrons in the outermost subshell. It therefore has a doublet and a quartet system, i.e. $S=1/2$ and $S=3/2$ (Fig. 17.4). Given the possible combinations of the quantum numbers m_l for the three p electrons of the configuration $1s^2 2s^2 2p^3$, the overall state can be either ^2P, ^2D or ^4S. Of these, the one with the lowest energy is ^4S, which is the state with the highest multiplicity. The other two states actually occur at somewhat higher energy in the doublet part of the nitrogen term scheme (Fig. 17.4).

3) When the highest value of the quantum number S is reached, the Pauli principle requires that the electrons be distributed among the substates m_l in such a way that $L_z = \sum m_l \hbar = m_L \hbar$ is maximised. The resulting angular momentum quantum number L is then equal to $|m_L|$. For a given multiplicity S, the higher values of L give states of lower energy.

4) Finally, when the spin-orbit coupling is also taken into account, the terms with the smallest quantum numbers J have the lowest energy in "normal" multiplets, but otherwise the converse holds. "Normal" means here that the subshells are less than half full.

This rule is a consequence of the fine structure calculation which was carried out earlier for the one-electron atom (Sect. 12.8). As the negative charge circulates around the positive nucleus, the orbital magnetic field at the position of the electron is directed in such a way that an antiparallel orientation of $\boldsymbol{L}$ and $\boldsymbol{S}$ corresponds to a minimum energy. If the shell is more than half full, however, each electron which would be needed to fill the shell is equivalent to a positively charged "hole". The sign of the magnetic field $\boldsymbol{B}_L$ then changes, and the state with the highest J has the lowest energy. In Fig. 19.4 this is shown by comparison of the one-electron atom lithium (ground state $^2S_{1/2}$) and the "one-hole" atom fluorine (ground state $^2P_{3/2}$).

The carbon atom can serve as an example here. Its term scheme is shown in Fig. 17.5. In the ground state, the carbon atom has two electrons in the outermost subshell. It therefore has a singlet and a triplet system with $S=0$ and $S=1$. The possible ground states for the electronic configuration $1s^2 2s^2 2p^2$ are ^1S, ^1D and ^3P. Because it has the largest multiplicity, ^3P has the lowest energy, as can also be seen in Fig. 17.5. If the angular momentum quantum number J is included, the possibilities are $^3P_0$, $^3P_1$ and $^3P_2$, i.e. $J=0, 1$ and 2. In a "normal" order of terms, the state $^3P_0$ has the lowest energy, by rule 4. The singlet terms are also observed, at somewhat higher energy, as the term scheme in Fig. 17.5 and Fig. 19.5 shows.

In the oxygen atom, however, the possible ground states for the $1s^2 2s^2 2p^4$ configuration are ^1S, ^1D and ^3P. According to rule 2, ^3P has the lowest energy. Now, however, with an inverted term order, the state with the largest value of J (rule 4) has the very lowest energy. The ground state is therefore $^3P_2$.

Table 19.3 contains the LS-ground state terms which are actually observed for all atoms. When the atomic number Z becomes large, they can often not be simply derived from the electron configurations, as they can near the beginning of the Periodic Table.

19.3 Excited States of Atoms and Possible Electronic Configurations. Complete Term Schemes

Several complete term schemes for atoms have already been shown in the figures. Each of the energy terms indicated there corresponds to a particular electron configuration and to a certain type of coupling of the electrons in non-filled shells. The energetic positions of these terms are uniquely determined by the energies of interaction between the nucleus and electrons and between the electrons, themselves. Quantitative calculations are extremely difficult, because atoms with more than one electron are complicated "many-particle" systems.

However, using a few examples, we shall consider how many different terms are possible for a given electronic configuration and how these are arranged energetically.

Our first example is an atom with two *p* electrons in unfilled shells, in the configuration $(np)^1(n'p)^1$. If $n = n'$, the two electrons are equivalent and the configuration is np^2. Carbon is a concrete example of this case.

Figure 19.5 shows the terms discussed already in Sect. 19.2 which are possible if the two *p* electrons are coupled. First of all, the two spins can be either parallel or antiparallel. The position functions associated with these alignments differ with respect to Coulomb repulsion, so that according to Hund's rule, the state with the spin quantum number $S = 1$ has a lower energy. Thus one obtains an $S = 1$ (triplet) and an $S = 0$ (singlet) term scheme, with the triplet scheme having lower energies. In addition, the orbital angular momenta $l_1 = 1$ and $l_2 = 1$ can couple to give $L = 2$, 1 and 0. This produces a *D*, a *P* and an *S* state. The state with the highest value of *L* has the lowest energy. This, like the other Hund rules, is not adequately understandable by intuition alone.

For the triplet terms ^3P and ^3D, the spin-orbit interaction leads to a further splitting into three states each. The singlet terms and the ^3S term are not subject to fine structure splitting, as we have seen earlier. Thus we obtain, in all, 10 spectral terms. In an external magnetic field, all those terms which have a total angular momentum $\boldsymbol{J}$ not equal to zero are further split into the m_J states. The terms indicated by dashed lines in Fig. 19.5 are not possible for equivalent electrons (i.e. in the np^2 configuration) due to the Pauli principle. Since the quantum numbers *n* and *l* are the same for the two electrons in these configurations, they must differ in their m_l or m_s quantum numbers. In this case, the terms ^1P, ^3S and ^3D would disobey the Pauli principle, and they are thus forbidden for equivalent electrons. For these terms, it is impossible to construct an antisymmetrical wavefunction for two *p* electrons with the same principal quantum number *n*.

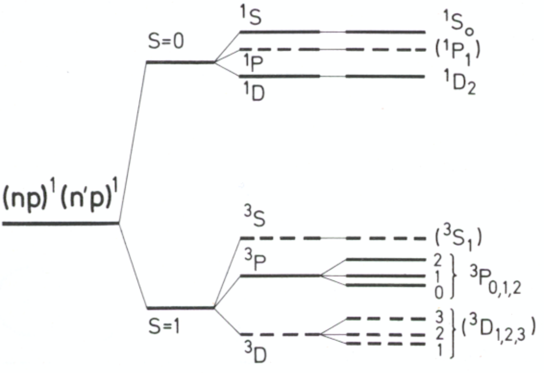

Fig. 19.5. Coupling of two *p* electrons. If the two electrons are equivalent (np^2 configuration), the terms indicated by dashed lines are forbidden by the Pauli principle. The presence of an external magnetic field lifts the *J* degeneracy and leads to further splitting of the terms, which is not shown here

For two non-equivalent s electrons, i.e. for the configuration $(ns)^1(n's)^1$, the only possible spectral terms are $^3S_1$ and $^1S_0$. For the configuration $(nd)^1(n'p)^1$, $^1P_1$, $^1D_2$, $^1F_3$, $^3P_{0,1,2}$, $^3D_{1,2,3}$ and $^3F_{2,3,4}$ are possible. It is left to the reader to confirm this. For heavy atoms, LS coupling is replaced by jj coupling.

In the general case, the possible atomic terms for a given configuration of equivalent or nonequivalent electrons can be obtained in the following manner: only the electrons in open shells (n,l) must be considered. Each electron, denoted by the index i, is characterised by the four quantum numbers, n_i, l_i, m_{li}, and m_{si}. These can be determined by applying a hypothetical magnetic field which is so strong that all the magnetic couplings are removed. According to *Ehrenfest*, a virtual, infinitely slow (adiabatic) change in the coupling conditions leaves the quantum numbers unchanged, and in particular, the number of terms remains constant in this case.

In order to derive all the possible terms, we have to consider all the possible variations of the couplings. The following rules hold:

- For each value of L, we have for $M_L = \Sigma m_{li}$ the possible values $L, L-1, \ldots -L$ for the component of the total orbital angular momentum parallel to the applied field;
- Likewise, for each S, we have the possible values $M_S = S, S-1, \ldots -S = \Sigma m_{si}$;
- When the electrons are completely decoupled by a strong magnetic field, the individual electrons are quantised according to $m_l = l, l-1, \ldots -l$ and $m_s = \pm\frac{1}{2}$.

Using these rules, one can write down all the possible electronic configurations (taking the Pauli principle into account). Table 19.4 shows this for the case of an np^4 configuration. One starts with the highest value of M_L, which corresponds to the highest possible L-value. In the case shown in the table, this is $M_L = 2$, with $M_S = 0$; the corresponding term is thus ^{1}D. It also corresponds to four additional configurations. The next highest value of M_L is $M_L = 1$, with the largest M_S-value being $M_S = 1$; the

Table 19.4. Possible Russell-Saunders terms for the electron configuration (np^4). The table is intended only to demonstrate the counting of the possible orientations of M_L and M_S from the allowed combinations of the one-electron quantum numbers m_l and m_s (indicated by arrows). If one wishes to construct the wavefunctions belonging to the quantum numbers, it is necessary to formulate singlet and triplet functions from the four possible arrangements. (↓↓, ↑↓, ↓↑, ↓↓) of two unpaired spins. More details are given in Sect. 19.4.2

$m_l = 1$	$m_l = 0$	$m_l = -1$	M_L	M_S	Term symbol
↑↓	↑↓		2	0	
↑↓	↑	↓	1	0	
↑	↑↓	↓	0	0	^{1}D
↑	↓	↑↓	−1	0	
	↑↓	↑↓	−2	0	
↑↓	↑	↑	1	1	
↑↓	↓	↑	1	0	
↑↓	↓	↓	1	−1	
↑	↑↓	↑	0	1	
↓	↑↓	↑	0	0	^{3}P
↓	↑↓	↓	0	−1	
↑	↑	↑↓	−1	1	
↓	↑	↑↓	−1	0	
↑	↓	↑↓	−1	−1	
↑↓		↑↓	0	0	^{1}S

corresponding ^{3}P term contains all together 9 configurations. Finally, only one configuration remains, namely that corresponding to ^{1}S. Therefore, four equivalent *p*-electrons yield the terms ^{1}D, ^{3}P, and ^{1}S, and no others, since only thus is a unique correspondence between terms and configurations achieved.

All those terms which arise from allowed electronic configurations of the atom are given in the term schemes, for example those in Fig. 17.4, 5. Together with the selection rules for optical transitions

$$\begin{array}{ll}
\Delta J = 0, \pm 1 & [\text{except for } (J = 0) \rightarrow (J = 0)] \\
\Delta m_J = 0, \pm 1 & [\text{except for } (m_J = 0) \rightarrow (m_J = 0) \text{ where } \Delta J = 0] \\
\multicolumn{2}{l}{\left.\begin{array}{l} \left.\begin{array}{l} \Delta S = 0 \\ \Delta L = 0, \pm 1 \end{array}\right\} \text{for the atom} \\ \Delta l = \pm 1 \text{ for the electron changing its configuration} \end{array}\right\} \text{in } LS \text{ coupling}} \\
\multicolumn{2}{l}{\Delta j = 0, \pm 1 \text{ for one of the electrons in } jj \text{ coupling}\,,}
\end{array}$$

the term schemes and the spectra of all atoms are understandable.

19.4 The Many-Electron Problem. Hartree-Fock Method*

19.4.1 The Two-Electron Problem

In Chap. 10, we were able to solve exactly the hydrogen problem, in which only a single electron orbits the nucleus. Unfortunately, there is no exact solution for any other atom with more than one electron. In spite of this, it is possible, usually to a very good approximation, to calculate wavefunctions and energies. In order to demonstrate the problems which arise here, we shall consider an atom with two electrons, for example the helium atom or a multiply ionised atom in which only two electrons remain (Fig. 19.6). We distinguish the coordinates of the two electrons by using the subscripts $j = 1$ or $j = 2$. If only one electron were present, the Hamiltonian would be

$$\mathscr{H}_j = -\frac{\hbar^2}{2m_0}\nabla_j^2 - \frac{Ze^2}{4\pi\varepsilon_0 r_j}\,, \tag{19.2}$$

where the Laplace operator is defined by

$$\nabla_j^2 = \frac{\partial^2}{\partial x_j^2} + \frac{\partial^2}{\partial y_j^2} + \frac{\partial^2}{\partial z_j^2}\,. \tag{19.3}$$

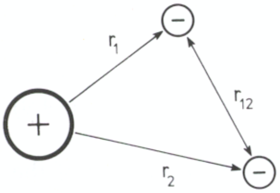

Fig. 19.6. Atom with two electrons

If we ignore the interactions between the electrons, in a *classical* treatment the energy of the whole system of two electrons is simply equal to the energy of the individual electrons. The Hamiltonian of the whole system is thus equal to the sum of the Hamiltonians of the two electrons. If we make use of the translation rule of quantum theory, which says that the kinetic energy is always to be replaced by the Laplacian (19.3), multiplied by $-\hbar^2/2m_0$, we obtain for the two-electron system the Hamiltonian

$$\mathcal{H}^0 = \mathcal{H}_1 + \mathcal{H}_2 , \tag{19.4}$$

where the Hamiltonian (19.2) is used. Actually, however, there is a direct interaction between the electrons. The most important part of this is the Coulomb interaction energy, so that we must replace (19.4) by

$$\mathcal{H} = \mathcal{H}_1 + \mathcal{H}_2 + \frac{e^2}{4\pi\varepsilon_0 r_{12}} , \tag{19.5}$$

where r_{12} is the distance between the two electrons. Our problem is to find an exact solution to the Schrödinger equation belonging to (19.5). As we remarked above, this is not possible in closed form. Therefore, we first consider the simpler problem in which the Coulomb interaction between the two electrons is left out and the Hamiltonian (19.4) is used in the Schrödinger equation. We make use of the fact that the single-particle Schrödinger equation with the Hamiltonian (19.2) has already been solved. In order to stay closer to reality, we include the spin of the electron and introduce the spin variable along with the position vector $\boldsymbol{r}_k$. As an abbreviation, we use the variable $\boldsymbol{R}_k$, which is defined as

$$\boldsymbol{R}_k = (\boldsymbol{r}_k, \text{spin variable}) \equiv (\boldsymbol{r}_k, k) . \tag{19.6}$$

As we saw in Chap. 10, the wavefunction of the one-electron problem is characterised by the quantum numbers n, l, m_l, and m_s: Ψ_{n,l,m_l,m_s}. The energy of this function is E_{n,l,m_l,m_s}. We now consider the Schrödinger equation for the total Hamiltonian (19.4):

$$\mathcal{H}^0 \Psi = E_t \Psi , \tag{19.7}$$

where E_t is an abbreviation for E_{tot}. Since the Hamiltonian $\mathcal{H}^0$ (19.4) includes the two variables $\boldsymbol{R}_1$ and $\boldsymbol{R}_2$, the wavefunction must naturally depend on these variables: $\Psi(\boldsymbol{R}_1, \boldsymbol{R}_2)$. In order to avoid writing out the quantum numbers explicitly in each of the following expressions, we introduce the abbreviation Q for the total set of quantum numbers,

$$Q = (n, l, m_l, m_s) \equiv (q, m_s) . \tag{19.8}$$

The Schrödinger equation (19.7) is solved by the wavefunction

$$\Psi(\boldsymbol{R}_1, \boldsymbol{R}_2) = \Psi_{Q_1}(\boldsymbol{R}_1)\, \Psi_{Q_2}(\boldsymbol{R}_2) , \tag{19.9}$$

as can be immediately demonstrated by substitution. The Ψ's on the right side of the equation are solutions for the one-particle Schrödinger equations. The total energy is, as can also be easily demonstrated,

$$E_t = E_{Q_1} + E_{Q_2}\,, \tag{19.10}$$

where the energies E on the right side are the one-particle energies associated with the quantum numbers Q_1 and Q_2. It would thus appear that we have reproduced, with no limitations, the above-mentioned classical result, that the one-particle energies are simply additive, if we ignore the electron interactions.

The solution (19.9) also appears to allow the case of $Q_1 = Q_2$, which would mean that the two electrons would have exactly the same four quantum numbers. According to the Pauli principle, however, this case is excluded. Theoretical physicists have therefore considered whether a wavefunction can be found which automatically excludes this case. To find it, we make use of the fact that not only (19.9), but also the wavefunction

$$\Psi_{Q_2}(\boldsymbol{R}_1)\,\Psi_{Q_1}(\boldsymbol{R}_2) \tag{19.11}$$

satisfies the Schrödinger equation (19.7), and yields exactly the same energy (19.10) as (19.9). As we know, any linear combination of wavefunctions which have the same energy is also a solution of the Schrödinger equation and has the same energy. The linear combination which automatically fulfils the Pauli principle is a difference between (19.9) and (19.11), namely

$$\Psi(\boldsymbol{R}_1,\boldsymbol{R}_2) = \frac{1}{\sqrt{2}}\,[\Psi_{Q_1}(\boldsymbol{R}_1)\,\Psi_{Q_2}(\boldsymbol{R}_2) - \Psi_{Q_2}(\boldsymbol{R}_1)\,\Psi_{Q_1}(\boldsymbol{R}_2)]\,. \tag{19.12}$$

This wavefunction vanishes identically if $Q_1 = Q_2$. The factor $1/\sqrt{2}$ serves to normalise the whole wavefunction. If we exchange the coordinates $\boldsymbol{R}_1$ and $\boldsymbol{R}_2$ in (19.12), the wavefunction is obviously converted to its additive inverse, or in other words, the wavefunction is *antisymmetric*. This is now a formulation which makes possible a statement of the Pauli principle even when there is interaction between the electrons: *The wavefunction must be antisymmetric with respect to the coordinates* $\boldsymbol{R}_1$ *and* $\boldsymbol{R}_2$. It should be remembered that the variables $\boldsymbol{R}_j$ include the spin variables.

Let us now investigate the rôle of the spin variables and of the corresponding spin wavefunctions.

To this end, we separate the total set of quantum numbers Q_k defined in (19.8) into

$$Q_k = (q_k, m_{s,k})\,, \tag{19.13}$$

as well as separating the variables $\boldsymbol{R}_k$ as in (19.6).

We now write the wavefunction $\Psi_{Q_k}(\boldsymbol{R}_k)$ as the product of a wavefunction $\psi_{q_k}(\boldsymbol{r}_k)$ for the orbital motion (space function) and a spin wavefunction $\phi_{m_{s,k}}(k)$ (spin function). We then have instead of (19.12)

$$\begin{aligned}\Psi(\boldsymbol{R}_1,\boldsymbol{R}_2) = \frac{1}{\sqrt{2}}\,(&\psi_{q_1}(\boldsymbol{r}_1)\,\psi_{q_2}(\boldsymbol{r}_2)\,\phi_{m_{s,1}}(1)\,\phi_{m_{s,2}}(2)\\ &-\psi_{q_1}(\boldsymbol{r}_2)\,\psi_{q_2}(\boldsymbol{r}_1)\,\phi_{m_{s,1}}(2)\,\phi_{m_{s,2}}(1)).\end{aligned} \tag{19.14}$$

For simplicity, we characterise the spin quantum numbers $m_s = \pm\frac{1}{2}$ by ↑ (spin up) or ↓ (spin down). We then find the following possibilities:

$$1) \quad m_{s,1} = \uparrow \ , \qquad m_{s,2} = \uparrow \tag{19.15}$$

$$2) \quad m_{s,1} = \downarrow \ , \qquad m_{s,2} = \downarrow \tag{19.16}$$

$$3) \quad m_{s,1} = \uparrow \ , \qquad m_{s,2} = \downarrow \tag{19.17}$$

$$4) \quad m_{s,1} = \downarrow \ , \qquad m_{s,2} = \uparrow \ . \tag{19.18}$$

In the wavefunctions belonging to 1) and 2), we can factor out the spin functions and obtain

$$1) \ \Psi_{\uparrow\uparrow}(\boldsymbol{R}_1, \boldsymbol{R}_2) = \frac{1}{\sqrt{2}}(\psi_{q_1}(\boldsymbol{r}_1)\,\psi_{q_2}(\boldsymbol{r}_2) - \psi_{q_1}(\boldsymbol{r}_2)\,\psi_{q_2}(\boldsymbol{r}_1)) \times \phi_\uparrow(1)\,\phi_\uparrow(2) \tag{19.19}$$

and

$$2) \ \Psi_{\downarrow\downarrow}(\boldsymbol{R}_1, \boldsymbol{R}_2) = \frac{1}{\sqrt{2}}(\psi_{q_1}(\boldsymbol{r}_1)\,\psi_{q_2}(\boldsymbol{r}_2) - \psi_{q_1}(\boldsymbol{r}_2)\,\psi_{q_2}(\boldsymbol{r}_1)) \times \phi_\downarrow(1)\,\phi_\downarrow(2) \ . \tag{19.20}$$

The wavefunction for two electrons may be written as a product of the space function and the spin function:

$$\Psi(\boldsymbol{R}_1, \boldsymbol{R}_2) = \psi(\boldsymbol{r}_1, \boldsymbol{r}_2)\,\Phi(1,2) \ , \quad \text{where} \tag{19.21}$$

$$\Phi_{\uparrow\uparrow}(1,2) = \phi_\uparrow(1)\,\phi_\uparrow(2) \quad \text{and} \tag{19.22}$$

$$\Phi_{\downarrow\downarrow}(1,2) = \phi_\downarrow(1)\,\phi_\downarrow(2) \ . \tag{19.23}$$

Let us consider the precise meaning of the spin wavefunctions Φ. Since they refer to two electrons, it seems reasonable of inquire into the total spin of the pair of electrons. The z component of the latter corresponds to the operator

$$\Sigma_z \equiv \sigma_{z,1} + \sigma_{z,2} \tag{19.24}$$

where $\sigma_{z,k}$ is the operator for the z component of the spin of electron k. As one can quickly verify, the following relations hold:

$$\Sigma_z \phi_\uparrow(1)\,\phi_\uparrow(2) = \hbar\,\phi_\uparrow(1)\,\phi_\uparrow(2) \quad \text{and} \tag{19.25}$$

$$\Sigma_z \phi_\downarrow(1)\,\phi_\downarrow(2) = -\hbar\,\phi_\downarrow(1)\,\phi_\downarrow(2) \ , \tag{19.26}$$

i.e. the spin functions (19.22, 23) are eigenfunctions of (19.24). Likewise, one can verify (cf. Problem 19.8) that they are simultaneously eigenfunctions of

$$\Sigma^2 \equiv (\boldsymbol{\sigma}_1 + \boldsymbol{\sigma}_2)^2 \tag{19.27}$$

with the eigenvalue $2\hbar^2$.

Let us now return to the possible spin arrangements (19.15 – 18) and write down the remaining wavefunctions which correspond to (19.17, 18):

$$3)\ \Psi(\boldsymbol{R}_1, \boldsymbol{R}_2) = \frac{1}{\sqrt{2}} (\psi_{q_1}(\boldsymbol{r}_1)\, \psi_{q_2}(\boldsymbol{r}_2)\, \phi_\uparrow(1)\, \phi_\downarrow(2) - \psi_{q_1}(\boldsymbol{r}_2)\, \psi_{q_2}(\boldsymbol{r}_1)\, \phi_\uparrow(2)\, \phi_\downarrow(1)) \tag{19.28}$$

$$4)\ \Psi(\boldsymbol{R}_1, \boldsymbol{R}_2) = \frac{1}{\sqrt{2}} (\psi_{q_1}(\boldsymbol{r}_1)\, \psi_{q_2}(\boldsymbol{r}_2)\, \phi_\downarrow(1)\, \phi_\uparrow(2) - \psi_{q_1}(\boldsymbol{r}_2)\, \psi_{q_2}(\boldsymbol{r}_1)\, \phi_\downarrow(2)\, \phi_\uparrow(1))\ . \tag{19.29}$$

These may evidently *not* be written in the form of products (19.21). However, as we know, we may take linear combinations of wavefunctions which belong to the same energy; in fact we must do so when applying perturbation theory to degenerate states. We thus take the sum of 3) and 4) and obtain after rearranging

$$\begin{aligned} 5) = 3) + 4) = &\ \frac{1}{2} (\psi_{q_1}(\boldsymbol{r}_1)\, \psi_{q_2}(\boldsymbol{r}_2) - \psi_{q_1}(\boldsymbol{r}_2)\, \psi_{q_2}(\boldsymbol{r}_1)) \times (\phi_\uparrow(1)\, \phi_\downarrow(2) + \phi_\uparrow(2)\, \phi_\downarrow(1)) \\ = &\ \Psi_{\uparrow\downarrow+\downarrow\uparrow}(\boldsymbol{R}_1, \boldsymbol{R}_2) \end{aligned} \tag{19.30}$$

and

$$\begin{aligned} 6) = 3) - 4) = &\ \frac{1}{2} (\psi_{q_1}(\boldsymbol{r}_1)\, \psi_{q_2}(\boldsymbol{r}_2) + \psi_{q_1}(\boldsymbol{r}_2)\, \psi_{q_2}(\boldsymbol{r})) \times (\phi_\uparrow(1)\, \phi_\downarrow(2) - \phi_\uparrow(2)\, \phi_\downarrow(1)) \\ = &\ \Psi_{\uparrow\downarrow-\downarrow\uparrow}(\boldsymbol{R}_1, \boldsymbol{R}_2)\ . \end{aligned} \tag{19.31}$$

These new wavefunctions thus indeed have the desired form (19.21) and are furthermore eigenfunctions of Σ_z and Σ^2:

$$\Sigma_z(\phi_\uparrow(1)\, \phi_\downarrow(2) \pm \phi_\uparrow(2)\, \phi_\downarrow(1)) = 0 \tag{19.32}$$

$$\Sigma^2(\phi_\uparrow(1)\, \phi_\downarrow(2) + \phi_\uparrow(2)\, \phi_\downarrow(1)) = 2\,\hbar^2(\phi_\uparrow(1)\, \phi_\downarrow(2) + \phi_\uparrow(2)\, \phi_\downarrow(1)) \tag{19.33}$$

$$\Sigma^2(\phi_\uparrow(1)\, \phi_\downarrow(2) - \phi_\uparrow(2)\, \phi_\downarrow(1)) = 0\ . \tag{19.34}$$

Clearly, the wavefunction

$$\Phi = \phi_\uparrow(1)\, \phi_\downarrow(2) - \phi_\uparrow(2)\, \phi_\downarrow(1) \tag{19.35}$$

corresponds to a singlet state ($S = 0$), while the spin wave-functions

$$\Phi = \begin{cases} \phi_\uparrow(1)\, \phi_\uparrow(2) & (19.36) \\ \phi_\uparrow(1)\, \phi_\downarrow(2) + \phi_\uparrow(2)\, \phi_\downarrow(1) & (19.37) \\ \phi_\downarrow(1)\, \phi_\downarrow(2) & (19.38) \end{cases}$$

correspond to a triplet state ($S = 1$) with $M_{s,z} = 1, 0, -1$.

The corresponding space functions, which are the wavefunctions for the orbital motion, have differing symmetries with respect to the space coordinates in the singlet and the triplet states.

The triplet state has antisymmetric space functions; thus, the probability density for both electrons being in the same place vanishes, and it becomes small when the electrons approach each other. The positive Coulomb repulsion energy between the electrons is thus lower for the triplet state than for the singlet state, which has a space function symmetric in the space coordinates. This forms the theoretical basis for Hund's rules (see Sect. 19.2).

19.4.2 Many Electrons Without Mutual Interactions

The considerations which led us to the wave function (19.12) can be generalised. We shall give the results here without proof. In the general case, we are concerned with the variables $\boldsymbol{R}_1, \dots \boldsymbol{R}_N$ of N electrons. In the absence of interactions among the electrons, the Hamiltonian is a sum of one-electron Hamiltonians:

$$\mathscr{H}^0 = \sum_{j=1}^{N} \mathscr{H}_j \, . \tag{19.39}$$

The solution of the Schrödinger equation

$$\mathscr{H}^0 \Psi = E_t \Psi \tag{19.40}$$

associated with (19.39) is naturally a function of the coordinates $\boldsymbol{R}_1, \dots \boldsymbol{R}_N$:

$$\Psi(\boldsymbol{R}_1, \boldsymbol{R}_2, \dots \boldsymbol{R}_N) \, . \tag{19.41}$$

Retaining the notation introduced above, we can immediately show that the Schrödinger equation (19.40) is solved by the product

$$\Psi(\boldsymbol{R}_1, \boldsymbol{R}_2, \dots \boldsymbol{R}_N) = \Psi_{Q_1}(\boldsymbol{R}_1)\, \Psi_{Q_2}(\boldsymbol{R}_2) \dots \Psi_{Q_N}(\boldsymbol{R}_N) \, . \tag{19.42}$$

This approach is often called the Hartree method. The energy of the solution is given by

$$E_t = E_{Q_1} + E_{Q_2} + \dots + E_{Q_N} \, , \tag{19.43}$$

where the energies on the right side are again the energies of the individual electrons.

The solution (19.42) is not yet compatible with the Pauli principle, because it allows solutions $Q_i = Q_k$ for the pair i, k. The solution which is compatible with the Pauli principle is given by a determinant of the form

$$\Psi(\boldsymbol{R}_1, \boldsymbol{R}_2, \dots \boldsymbol{R}_N) = \frac{1}{\sqrt{N!}} \begin{vmatrix} \Psi_{Q_1}(\boldsymbol{R}_1)\, \Psi_{Q_1}(\boldsymbol{R}_2) & \dots \Psi_{Q_1}(\boldsymbol{R}_N) \\ \Psi_{Q_2}(\boldsymbol{R}_1)\, \Psi_{Q_2}(\boldsymbol{R}_2) & \dots \\ \vdots & \\ \Psi_{Q_N}(\boldsymbol{R}_1)\, \Psi_{Q_N}(\boldsymbol{R}_2) \dots & \Psi_{Q_N}(\boldsymbol{R}_N) \end{vmatrix} \, . \tag{19.44}$$

A determinant changes its sign if two rows or two columns are exchanged. If we exchange two variables $\boldsymbol{R}_i$ and $\boldsymbol{R}_k$, this is equivalent to exchanging two columns in (19.44). Thus (19.44) guarantees the antisymmetry of the wavefunction. Since a determinant is zero if any two rows or columns are identical, we see that (19.44) vanishes if $Q_i = Q_k$ for any pair i, k.

We shall now discuss a special case of (19.44), namely the case that all the electrons have parallel spins. Then the spin quantum number m_s is e.g. 1/2 for all j. If we also ignore spin-orbit coupling, then the wavefunction of an individual electron can be written as a product (where we write m_k for the quantum number m_l):

$$\Psi_{Q_k}(\boldsymbol{R}_j) = \psi_{n_k, l_k, m_k}(\boldsymbol{r}_j) \cdot \phi_{\uparrow}(j) \tag{19.45}$$

where ψ refers to the orbital motion and ϕ to the spin. As can be shown using elementary rules for determinants, substitution of (19.44) in (19.45) yields

$$\Psi(\boldsymbol{R}_1, \dots \boldsymbol{R}_N) = \frac{1}{\sqrt{N!}} \begin{vmatrix} \psi_{n_1,l_1,m_1}(\boldsymbol{r}_1) \dots \psi_{n_1,l_1,m_1}(\boldsymbol{r}_N) \\ \vdots \\ \psi_{n_N,l_N,m_N}(\boldsymbol{r}_1) \end{vmatrix} \cdot \phi_{\uparrow}(1) \dots \phi_{\uparrow}(N) , \tag{19.46}$$

i.e. the total wavefunction is now a product of a spin function which is symmetric (because the spin quantum numbers of the electrons are identical) and an antisymmetric wavefunction, which is represented by a determinant as in (19.46) and depends only on the position variable $\boldsymbol{r}_j$.

If we set the coordinates for a pair i, k equal, $\boldsymbol{r}_i = \boldsymbol{r}_k$, in the determinant, it will of course vanish. This means that two electrons with parallel spins cannot occupy the same position. Since the wavefunction ψ is continuous, so is Ψ. This means that the probability of finding two electrons at the same position goes to zero continuously if the coordinates of the two become equal. The Pauli principle thus provides automatically for a certain distance between electrons with parallel spins.

19.4.3 Coulomb Interaction of Electrons. Hartree and Hartree-Fock Methods

We now turn to the actual problem, in which the Coulomb interaction among the electrons is taken into account. The energy of the Coulomb interaction between the pair of electrons j, k is given by $e^2/(4\pi\varepsilon_0 r_{jk})$ (r_{jk} is the distance between the two electrons), so the Hamiltonian is

$$\mathscr{H} = \sum_{j=1}^{N} \mathscr{H}_j + \sum_{j<k} \frac{e^2}{4\pi\varepsilon_0 r_{jk}} . \tag{19.47}$$

The summation rule $j<k$ prevents the interaction energy between pairs of electrons being counted twice. If instead of using this rule, we sum over all indices j and k, with the limitation that $j \neq k$, we must set a factor 1/2 in front of the interaction sum:

$$\mathscr{H} = \sum_{j=1}^{N} \mathscr{H}_j + \frac{1}{2} \sum_{j \neq k} \frac{e^2}{4\pi\varepsilon_0 r_{jk}} . \tag{19.48}$$

Our next task is to solve the Schrödinger equation

$$\mathscr{H}\Psi = E_t \Psi \tag{19.49}$$

for the Hamiltonian (19.48). Since there is no exact solution we follow this train of thought: First, since the one-electron problem has already been solved, the wavefunctions of the individual electrons, in the form

$$\Psi_Q(\boldsymbol{R}_j) \tag{19.50}$$

are already known. There is a charge density distribution associated with the wavefunction (19.50),

$$\varrho(\boldsymbol{r}_j) = e|\Psi_Q(\boldsymbol{R}_j)|^2 . \tag{19.51}$$

As we know from electrostatics, there is an interaction energy between a charge at position $\boldsymbol{r}$ and the charge distribution given by (19.51). This energy is given by the product of the charge and the electrostatic potential. The latter can be calculated from the charge distribution ϱ. In all, the Coulomb interaction energy is expressed by

$$V(\boldsymbol{r}) = \frac{1}{4\pi\varepsilon_0}\int\frac{e\varrho(\boldsymbol{r}_j)}{|\boldsymbol{r}-\boldsymbol{r}_j|}d\tau_j , \tag{19.52}$$

where the integral covers the total volume (the volume element is indicated here by $d\tau$, in order to distinguish it from the interaction energy V). If we substitute (19.51) in (19.52), we obtain

$$V(\boldsymbol{r}) = \frac{1}{4\pi\varepsilon_0}\int\frac{e^2|\Psi_Q(\boldsymbol{R}_j)|^2}{|\boldsymbol{r}-\boldsymbol{r}_j|}d\tau_j . \tag{19.53}$$

The main idea of the Hartree and Hartree-Fock methods, which are discussed below, is to reduce the many-electron problem to a one-electron problem. Let us consider a single electron. It is moving not only in the field of the atomic nucleus, but also in the field of all the other electrons. The simplifying assumption is then made that the electron density distribution of all the other electrons can be given, as a first approximation, by one-electron wavefunctions (19.50). In order to calculate the wavefunction of the chosen electron, we must solve a Schrödinger equation in which both the Coulomb potential of the nucleus and the interaction energy with all the other electrons appear. If the chosen electron has the subscript k, and thus the coordinate $\boldsymbol{R}_k$, the Schrödinger equation is

$$\left[-\frac{\hbar^2}{2m_0}\nabla_k^2-\frac{Ze^2}{4\pi\varepsilon_0 r_k}+V_k^{(0)}(\boldsymbol{r}_k)\right]\psi_k^{(1)}(\boldsymbol{R}_k) = E\psi_k^{(1)}(\boldsymbol{R}_k) . \tag{19.54}$$

$V_k^{(0)}$ is the Coulomb interaction energy with all the other electrons, and is obtained from

$$V_k(\boldsymbol{r}) = \sum_{j=1}^{N}{}'\int\frac{e^2|\psi_{Q_j}(\boldsymbol{R}_j)|^2}{4\pi\varepsilon_0|\boldsymbol{r}-\boldsymbol{r}_j|}d\tau_j \tag{19.55}$$

by substituting, as a first approximation, the wavefunction $\psi_{Q_j}^{(0)}$ for ψ_{Q_j} in (19.55)[1]. The

---

[1] The prime sign ($'$) on the sum in (19.55) indicates that $j \neq k$

superscript (0) means that we use a given (or guessed) wavefunction to start the whole procedure. In particular, $\psi_{Q_j}^{(0)}$ may be a wavefunction belonging to a given potential. Similarly, the superscript (1) indicates that this wavefunction for the electron k was obtained from (19.54) in the first step of an iterative process. In the second step, we now use the wavefunction $\psi^{(1)}$ for ψ in (19.55). This yields the new wavefunction $\psi^{(2)}$ in a Schrödinger equation analogous to (19.54). The process is repeated until there are no more significant changes in the wavefunctions $\psi^{(j)}$, or in other words, until the method converges. Seen schematically, we have

$$\psi^{(0)} \to V^{(0)} \to \psi^{(1)} \to V^{(1)} \to \psi^{(2)} \to V^{(2)} \dots \psi^{(j)} \to \psi \,. \tag{19.56}$$

The method described above is somewhat heuristic, of course. It is desirable to set it on a firm mathematical basis, which is possible, but we cannot go into the details here because of space limitations. It can be shown that the Schrödinger equation (19.49) may be solved by using a variational principle. According to this principle, the expression

$$\int \dots \int \psi^* \mathscr{H} \psi \, d\tau_1 \dots d\tau_N \tag{19.57}$$

must be equal to an extremum (maximum or minimum) with the secondary condition that the wavefunctions are normalised:

$$\int \Psi^* \Psi \, d\tau_1 \dots d\tau_N = 1 \,. \tag{19.58}$$

If we use a wavefunction Ψ of the form (19.42), i.e. a product wavefunction in such a variational procedure, we find a set of Schrödinger equations for the individual wavefunctions:

$$\left[-\left(\frac{\hbar^2}{2m_0}\right)\nabla_k^2 - \frac{Ze^2}{4\pi\varepsilon_0 r_k} + V_k(\boldsymbol{r}_k)\right]\psi_{Q_k}(\boldsymbol{R}_k) = E\psi_{Q_k}(\boldsymbol{R}_k)\,, \tag{19.59}$$

where $V_k(\boldsymbol{r}_k)$ is defined by (19.55). The Hartree method just consists of solving these Schrödinger equations (19.59) iteratively in the way indicated above.

The disadvantage of the Hartree method is obvious, in that it uses product trial functions for Ψ, which, as we know, violate the Pauli principle. The key to expanding the Hartree method to include the Pauli principle lies in utilising the determinant trial functions (19.44) for Ψ in the variation equations (19.57) and (19.58). The corresponding calculations are rather long; we shall therefore simply give the result here. For the individual wavefunctions, we find a set of Schrödinger equations of the form

$$\begin{aligned}&\left[-\left(\frac{\hbar^2}{2m_0}\right)\nabla_k^2 - \frac{Ze^2}{4\pi\varepsilon_0 r_k} + V_k(\boldsymbol{r}_k)\right]\psi_{Q_k}(\boldsymbol{R}_k)\\ &\quad - \sum_j{}' \frac{1}{4\pi\varepsilon_0}\int \psi_{Q_j}^*(\boldsymbol{R}_j)\,\frac{e^2}{|\boldsymbol{r}_k - \boldsymbol{r}_j|}\,\psi_{Q_k}(\boldsymbol{R}_j)\,d\tau_j \cdot \psi_{Q_j}(\boldsymbol{R}_k) = E\psi_{Q_k}(\boldsymbol{R}_k)\,.\end{aligned} \tag{19.60}$$

The term in brackets on the left-hand side, and the right-hand side of (19.60) agree with the Hartree equation (19.59). The additional term containing the sum over j is new; it is referred to as an exchange term. The reason for this terminology is the following: if one compares $V_k \cdot \psi_{Qk}$ from (19.60) with this exchange term, one recognises that the wavefunction ψ_{Qk} has exchanged rôles with the wavefunction ψ_{Qj}, since the electron coordinates $\boldsymbol{R}_k$ and $\boldsymbol{R}_j$ have been exchanged. This exchange term is a direct result of the determinant approach, i.e. of the antisymmetry of the wavefunctions. Intuitively explained, it means that the Coulomb interaction energy between electrons with parallel spins is reduced relative to that between electrons with antiparallel spins. Since the interaction potentials V themselves depend on the wavefunctions ψ, a solution to (19.60) is difficult to find. For a solution, one therefore resorts again to the Hartree-Fock method, according to which (19.60) is solved iteratively following the scheme (19.56).

Problems

19.1 How many electrons do those atoms have in which the following shells are filled in the ground state:

a) the K and the L shells, the $3s$ subshell and half the $3p$ subshell?
b) the K, L and M shells and the $4s$, $4p$ and $4d$ subshells?

What are the two elements in (a) and (b)?

19.2 Show that for a closed nl shell, $L = S = 0$.

19.3 a) Two equivalent p electrons have strong spin-orbit coupling. Calculate the possible values of the total angular momentum quantum number, if the coupling is purely jj. Remember to take the Pauli principle into account.

b) Consider the same problem in the case of weak spin-orbit coupling, so that LS coupling of the two p electrons can be assumed. Do the same values of $\boldsymbol{J}$ occur with equal frequency in the two cases?

Hint: Since the particles cannot be distinguished, configurations which are the same except for the exchange of electron indices may only be counted once. In case (a), the Pauli principle can be taken into account in this way, because the two electrons cannot have identical sets of quantum numbers. In case (b), the Pauli principle is taken into acount by the requirement that the wavefunction of the overall state must change its sign when the particle indices are exchanged (antisymmetry under particle exchange).

19.4 Give the terms for the following configurations and indicate in each case which term has the lowest energy:
(a) ns, (b) np^3, (c) $(np)^2(n's)$, (d) np^5, (e) $(nd^2)(n'p)$, (f) $(nd)(n'd)$.

19.5 In a diagram, show the occupied electronic states of the Si, Cl and As atoms when the atoms are in the ground state configurations.

In each case, write the electronic configuration and the terms of the ground state.

19.6 Give the ground state configuration and the number of unpaired electrons in the following atoms:

a) S
b) Ca
c) Fe
d) Br .

19.7 Calculate the terms for the np^3 configuration. Give the values of S, L and J for the terms

$$^1S_0,\ ^2S_{1/2},\ ^1P_1,\ ^3P_2,\ ^3F_4,\ ^5D_1,\ ^1D_2 \text{ and } ^6F_{9/2}\,.$$

Decide which of the terms correspond to the nd^2 configuration. Use your result to determine the ground and first excited states of titanium.

19.8 Demonstrate that the relations (19.25, 26), and (19.32) are correct. Show also that (19.35 – 38) are eigenfunctions of $\boldsymbol{\Sigma}^2$ and confirm the eigenvalues given in the chapter.

Hint: Write $\boldsymbol{\Sigma}^2$ as $(\boldsymbol{\sigma}_1 + \boldsymbol{\sigma}_2)^2 = \boldsymbol{\sigma}_1^2 + \boldsymbol{\sigma}_2^2 + 2\boldsymbol{\sigma}_1\boldsymbol{\sigma}_2$.

19.9 Is there a triplet state when the quantum numbers of the two electrons are identical? Justify your answer.

Hint: Consider the symmetry of the spatial wavefunction.